Modification of Forward Osmosis Membrane to Concentrate Protein

Weerapong Bootluck

A Thesis Submitted in Partial Fulfillment of the Requirements for the
Degree of Master of Science in Environmental Management
Prince of Songkla University
2015

Modification of Forward Osmosis Membrane to Concentrate Protein

Weerapong Bootluck

A Thesis Submitted in Partial Fulfillment of the Requirements for the
Degree of Master of Science in Environmental Management
Prince of Songkla University
2015

Thesis Title Modification of Forward Osmosis Membrane to Concentrate Protein

Author Mr. Weerapong Bootluck

Major Program Environmental Management

Major Advisor

....
(Dr. Watsa Khongnakorn)

Co-advisor

....
(Assoc. Prof. Dr. Wirote Youravong)

Examining Committee :

....Chairperson
(Dr. Chaiwat Rongsayamanount)

....Committee
(Ass. Prof. Dr. Chaisri Suksaroj)

....Committee
(Assoc. Prof. Dr. Galaya Srisuwan)

....Committee
(Dr. Watsa Khongnakorn)

....Committee
(Assoc. Prof. Dr. Wirote Youravong)

The Graduate School, Prince of Songkla University, has approved this thesis as partial fulfillment of the requirements for the Master of Science Degree in Environmental Management

....
(Assoc. Prof. Dr. Teerapol Srichana)
Dean of Graduate School

This is to certify that the work here submitted is the result of the candidate's own investigations. Due acknowledgement has been made of any assistance received.

....Signature
(Dr. Watsa Khongnakorn)
Major Advisor

....Signature
(Assoc. Prof. Dr. Wirote Youravong)
Co-advisor

....Signature
(Mr. Weerapong Bootluck)
Candidate

I hereby certify that this work has not been accepted in substance for any degree, and is not being currently submitted in candidature for any degree.

....Signature
(Mr. Weerapong Bootluck)
Candidate

ชื่อวิทยานิพนธ์ การปรับปรุงฟอร์เวิดออสโมซิสเมมเบรนเพื่อทำข้นโปรตีน
ผู้เขียน นายวีรพงค์ บุตรลักษณ์
สาขา การจัดการสิ่งแวดล้อม
ปีการศึกษา 2558

บทคัดย่อ

งานวิจัยนี้มีวัตถุประสงค์เพื่อปรับปรุงผิวเมมเบรนชนิด เซลลูโลสไตรอะซิเตท เพื่อทำข้นโปรตีนจากน้ำนึ่งปลาทูน่าด้วยเทคนิคพลาสมาในกระบวนการฟอร์เวิดออสโมสิส โดยศึกษาการปรับปรุงผิว เมมเบรนด้วยเทคนิค plasma treatment และเทคนิค plasma grafting polymerization จากการศึกษาพบว่าช่วงเวลาที่เหมาะสมที่สุดที่เวลา 10 วินาที ด้วยอาร์กอนพลาสมาดิสชาร์จ ที่กำลัง 20 วัตต์ ด้วยเทคนิค Ar plasma TiO_2 grafting polymerization (CTA;Ar+TiO_2) ผลจากการศึกษาคุณลักษณะความชอบน้ำ พบว่าค่ามุมสัมผัสของน้ำลดลงจาก 64.04±3.13 เป็น 27.43±0.24 องศา ศึกษาลักษณะความขรุขระของผิวเมมเบรนพบว่าเพิ่มสูงขึ้นจาก 5.04 ถึง 14.54 นาโนเมตร ตามลำดับ ศึกษาโครงสร้างหมู่ฟังก์ชันพบว่า กลุ่มคาร์บอกซิล (–COOH) ไฮดรอกซิล (-OH) ซึ่งเป็นกลุ่มที่ชอบน้ำเพิ่มสูงขึ้น ทดสอบประสิทธิภาพการซึมผ่านของน้ำเพิ่มสูงขึ้นจาก 0.74 ถึง 1.78 LMH ค่าฟลักซ์เพิ่มสูงขึ้นจาก 5.08 ถึง 9.22 LMH ค่าการกักกันเกลือเพิ่มขึ้นร้อยละ 91 ในขณะที่ค่าผันกลับของเกลือลดลงเท่ากับ 0.02 molMH ศึกษาผลของปัจจัยที่มีผลต่อค่าฟลักซ์พบว่า ความความเข้มข้นของสารละลายโซเดียมครอไรด์ (draw solution) ที่ 2 โมลาร์ เท่ากับ 6.11 LMH อัตราการไหลที่ 0.7 cm/s เท่ากับ 6.28 LMH และผลของอุณหภูมิที่ 45 องศา เท่ากับ 7.63 LMH พบว่าค่าฟลักซ์เพิ่มสูงขึ้นทุกปัจจัยการทดลอง แต่ในขณะเดียวกันค่าผันกลับของโซเดียมครอไรด์ (salt reverse flux) มีค่าเพิ่มขึ้น

การทำข้นโปรตีนจากน้ำนึ่งปลาทูน่า โดยใช้เมมเบรนชนิด CTA;Ar+TiO_2 พบว่าโปรตีนมีความเข้มข้นเพิ่มขึ้นร้อยละ 10.30 น้ำหนักต่อปริมาตร ความสามารถการนำกลับของโปรตีนเพิ่มขึ้นร้อยละ 87.3 เปอร์เซนต์ ค่าฟลักซ์เท่ากับ 5.38 LMH และค่าการผันกลับของเกลือลดลงเท่ากับ 0.14 gMH จากนั้นศึกษาส่วนประกอบของน้ำนึ่งปลาทูน่าหลังจากการกรองพบว่า ค่าซีโอดี (COD) เท่ากับ 1,955 มิลลิกรัมต่อลิตร ค่าบีโอดี (BOD) เท่ากับ 2.60 มิลลิกรัมต่อลิตร ค่าทีโอซี (TOC) ลดลงร้อยละ 50 ตามลำดับ

Thesis Title Modification of Forward Osmosis Membrane to Concentrate Protein
Author Mr. Weerapong Bootluck
Major Program Environmental Management
Academic Year 2015

ABSTRACT

This research aims at modifying the cellulose triacetate (CTA) membrane surface in order to concentrate the protein by using Forward Osmosis (FO). This study was to modify the membrane surface by using plasma treatment and plasma grafting polymerization, the optimizing of Ar plasma TiO_2 grafting polymerization (CTA;Ar+TiO_2) of 10 seconds at 20 watts. The results of modified CTA membrane indicated that the contact angle decreased from 64.04 + 3.13° to 27.43 ± 0.24°. The mean roughness (Ra) increased from 5.52 to 14.54 nm. The hydrophilic chemical functional groups like -COOH and –OH also increased. The performance of membrane, the water permeability increased from 0.74 to 1.78 LMH while the water flux increased from 5.05 to 9.22 LMH. The salt rejection increased up to 89-91 % whereas the reverse salt flux decreased to 0.02 molMH. The enhanced flux with the effect of operating condition was hereby studied. The feed solution NaCl 2 M as draw solution showed higher water flux at 6.11 LMH. The cross-low velocity at 0.7 cm/s showed higher flux at 6.28 LMH, and the higher temperature showed high water flux at 7.63 LMH at 45 ºC.

The protein was concentrated from tuna cooking juice by CTA;Ar+TiO_2 membrane. The concentration was 10.30 (w/v) %. The percentage of protein recovery was 87.3 %. While the water flux was 5.38 LMH, and the reverse salt flux was 0.14 gMH. For the physico-chemical characteristic of filtrated tuna cooking juice, it was found that COD was at 1,955 mg/L; BOD was at 2.60 mg/L; and TOC decreased 50 %, respectively.

Acknowledgement

I would like to thank my advisor, Dr. Watsa Khongnakorn. I would like to thank for her invaluable suggestion and lessons for my academic knowledge, guidance, kindness and assistant during my study. I would like to thank my co-advisor, Assoc Prof. Dr. Wirote Youravong. I also would like to thank for his guidance during my study.

I am also grateful to Faculty of Environmental Management, Prince of Songkla University, Membrane Science and Technology Research center (MSTRC), Faculty of Science, Prince of Songkla University and graduate school, Prince of Songkla University for finance support.

I would like to thank Dr. Chalad Yuenyao and Mr.Nikom Phuengkum from Department of Physic, Faculty of Science, Prince of Songkla University, for their guidance and helpful suggestion.

I would like thank to all lecture at Faculty of Environmental Management, Prince of Songkla University, for their kindness help.

I would like to thank my family for their support during my study.

Weerapong Bootluck

Contents

Chapter

Contents (Continued)

Contents (Continued)

Page

Contents (Continued)

List of Tables

List of Figures

List of Figures (Continued)

List of Figures (Continued)

List of Abbreviations

A	water permeability coefficient (LMH)
B	Salt permeability coefficient (LMH)
C	Concentration, M;
Cp	Concentration of permeate
Cf	Concentration of feed
CP	Concentration polarization
CTA	Cellulose triacetate
CTA;CO_2	Carbon dioxide plasma treatment on cellulose triacetate
CTA;Ar	Argon plasma treatment on cellulose triacetate
CTA;Ar+AAc	Argon plasma acrylic acid grafting polymerization on cellulose triacetate
CTA;Ar+TiO_2	Argon plasma titanium dioxide grafting polymerization on cellulose triacetate
DS	Draw solution
ECP	External concentration polarization
FO	Forward osmosis
FS	Feed solution
ICP	Internal concentration polarization
MD	Membrane distillation
MF	Microfiltration
pI	Isoelectric point
UF	Ultrafiltration
R	% Salt rejection
RO	Reverse osmosis
J_w	Water flux (LMH)
π D,b	The osmotic pressure of draw solution
π F,b	The osmotic pressure of feed solution
ΔP	Pressure (bar)
$\Delta\pi$	Osmotic pressure (bar)
n	The number of ions dissociated of one salt molecule;

List of Abbreviations (Continued)

C	Concentration, M;
R	Universal gas constant (8.314kPa.l.mol-1.K-1);
T	Temperature, K

Chapter 1

Introduction and literature review

1.1 Background

Thailand is ranked the largest exporter of canned-tuna products in the world [1]. The canned tuna is the major industry in the south of the country. Its manufacturing process causes the solid waste and the liquid waste that produce high BOD loading to the wastewater treatment plants. Tuna cooking juice contains approximately 4 % valuable protein [2, 3]. The protein utilized from tuna cooking juice can be potentially used as a source of bioactive peptide, i.e. anti-oxidative, antimicrobial, antihypertensive, etc. [4-7]. There are many methods to separate the protein from tuna cooking juice such as precipitation, colloid gas aphrons (CGA), gel filtration chromatography, or membrane separation. [8-10]. However, membrane technology is preferably recommended for protein separation [4, 8].

Forward Osmosis (FO) is a process of membrane separating in which it establishes the natural driving force called osmotic pressure. FO process is quite advanced than other processes in term of lower membrane fouling, low hydraulic-pressure operation and cost energy consumption [11-13]. The FO process can be applied in food industry, desalination, wastewater treatment and power generation [14-17]. However, high reverse salt from draw solution in the performance of FO process is limited. Many researches attempt to modify the membrane surface for enhancing the water flux. The modification of membrane surface increases the hydrophilicity to enhance the flux and reduce the membrane fouling [12, 18, 19].

The plasma treatment is a method used to enhance the hydrophilicity of membrane surface. There are several methods of plasma treatment and plasma grafting polymerization to adjust the membrane surface such as hydrophilic of membrane surface and cross-linking hydrophilic polymer. In addition, the plasma treatment can improve functional group on polymer surface of hydrophilic membrane such as carboxylate groups to be lower fouling less hydrophobic membrane surface [12].

The objectives of this research include:

1. To modify membrane surface in order to enhance the flux and decrease the salt reverse flux.
2. To recover the protein from tuna cooking juice by using Forward Osmosis (FO) process with the membrane modification.

1.2 Literature review

1.2.1 Tuna canned industry

Canned tuna industry has become the major industry in Thailand. It produces almost 80 %, higher than all other canning industries in Thailand. Generally, Thailand produces and exports canned-tuna products more than 55,500 tons. Its export value reached approximately 86,446 million baht in 2013. Figure 1.1 shows the annual growth value of 19 % [1].

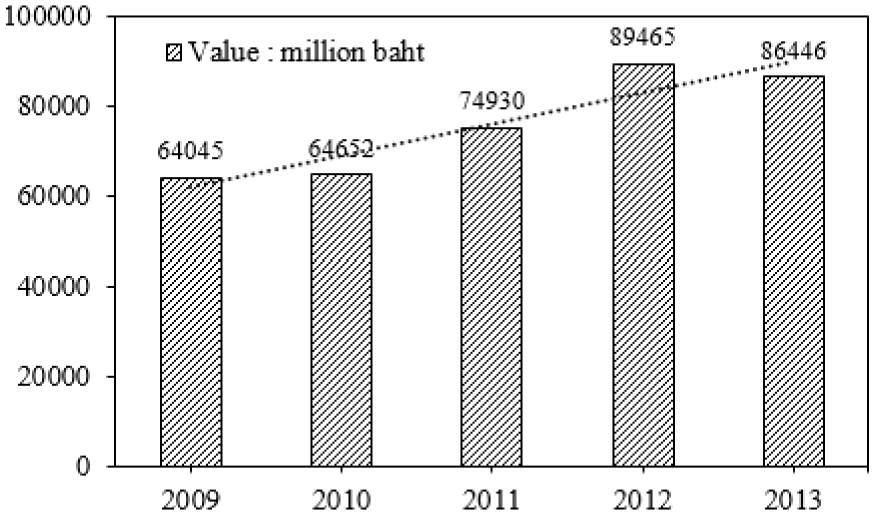

Figure 1.1. Thailand export value of canned-tuna products [1].

1.2.1.1 Canned tuna processes

The canned-tuna industry is the major industry in the south of Thailand. Specifically, canned-tuna process creates about 25 - 30 % of solid waste (e.g. head, skin, bone, and dark meat) and about 35% of liquid waste (e.g. water, oil, and tuna cooking juice). In addition, tuna cooking juice contains roughly 4 % of protein [2, 5, 8]. Figure 1.2 shows the flow chart process of canned-tuna and the waste from its process.

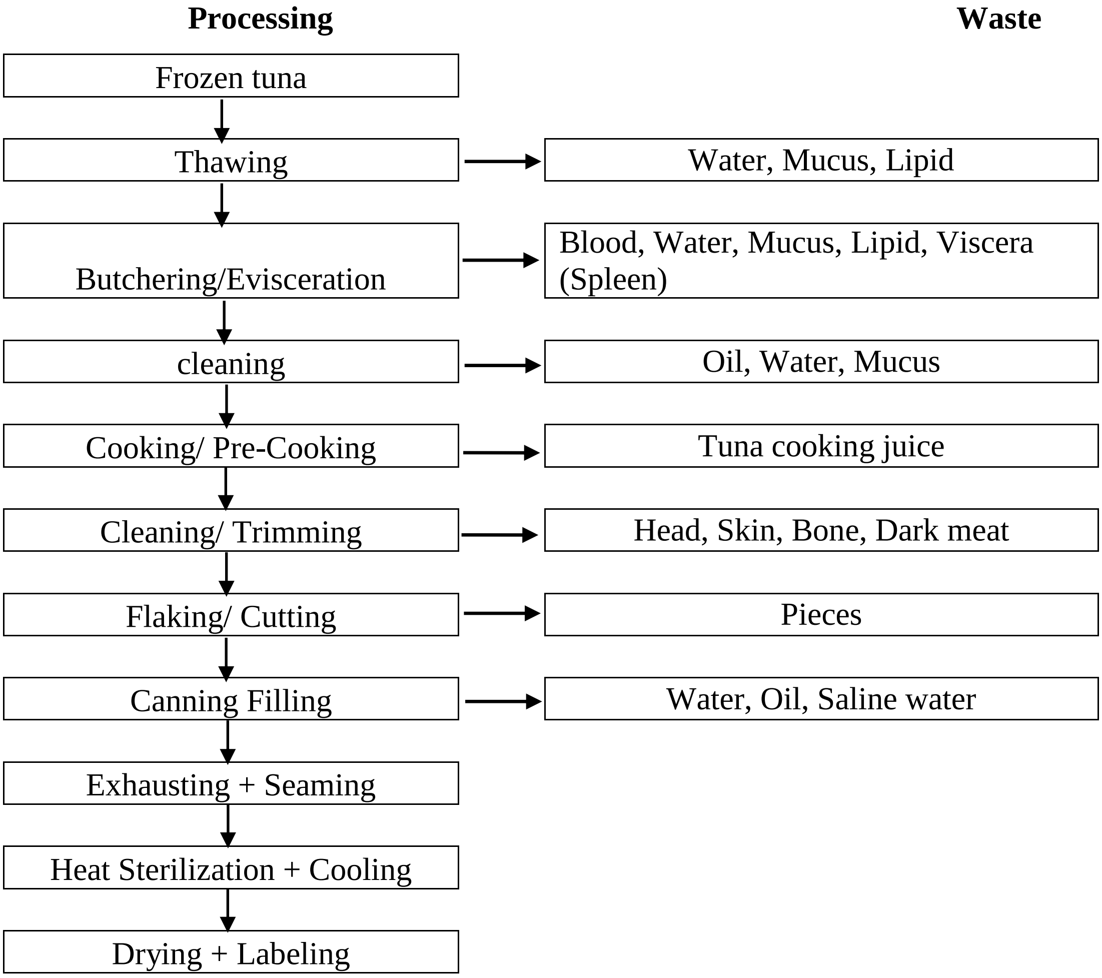

Figure 1.2. Typical flow chart of the tuna canning process [14].

1.2.1.2 Characteristic of tuna cooking juice.

Tuna cooking juice is the high concentrate of the compound of clouding protein, fat and others [3, 5] showed in Table 1.1. The protein in tuna cooking juice contains about 3.5 - 5.6 %, high concentrate about 68,450-82,800 mg/L of the chemical oxygen demand (COD), total solid about 73,200-82,800 mg/L. However, the recovery of protein is essential for decreasing wastewater which is loading and utilizing of available protein.

Table.1.1 Tuna cooking juice characteristic

Raw Material	pH	COD (mg/L)	Protein (%)	Total solid(mg/L)	Salt (%)	Fat (%)	Reference
Tuna cooking juice	5.91	19,000	3.51	-	-	-	[4]
	6.09	52,416	4.9	81,503		1.89	[33]
	6.07	49476	5.5	82,800	0.22	0.17	[34]
	6.07	73,617	4.15	68,450	-	-	[35]
	6.48	-	5.63	73,200	0.7	0.04	[36]

1.2.1.3 Utilization of protein recovery form tuna cooking juice

The utilization of protein has been reported as the method for recovering the concentrate of protein form tuna cooking juice. Recently, the market for protein production is rising up to 11.10 %, annually and globally, and the value is about 5 billion (US$) [24]. In addition, there are plenty of methods for recovering of protein such as precipitation, ion-exchang, gel filtration chromatography, freez-drying, spray-drying and evaporation [10]. The disadvantage of such methods is the contamination from chemicals and durations of protein from high temperature. Then the membrane process is a selected method for concentration and purification in food industry because its advantages are low operation cost, high production and no chemical contamination [8, 10].

Tuna cooking juice from tuna-caned industry process can be used to utilization of protein from tuna cooking juice. The protein can be used for developing new hydrolysis (e.g. inhibitory activities of angiotensin-I-converting enzyme (ACE), bioactive peptide, and antioxidative peptide). The protein hydrolysis can be beneficially used to protect human health. In addition, the membrane separation from tuna cooking juice can reduce the environmental pollutant caused from wastewater treatment [10]. M. Hajiham and W. Youravong (2013) [8] previously studied protein concentration and salt separation from tuna cooking juice by nanofiltration (NF) membrane, using cross-flow velocity of 800 L/h at 10 bar. It was found that the protein increased up to 10 % while the salt rejected about 70 %. The study was considered successful for concentrating high protein and rejecting salt. J. Kasiwut (2012) [5] also studied the concentration of protein from tuna cooking juice by ultrafiltration membrane, using hollow fiber membrane of 1 kDa and 5 kDa, pressure at 2.5 bar and cross-flow velocity of 2.7 cm/s. It showed the water flux of 6.85 LMH and 19.5 LMH. The protein concentration increased about 75 % and 87.5 % for membrane pore-size of 1 kDa and 5 kDa, respectively. Walha et al., (2009) [4] studied the separation of total solid from tuna cooking juice by nanofiltration membrane, using pressure at 35 bar. The result was that the COD decreased from 63,000 mg/L to 1,900 mg/L. It significantly decreased about 72 %. A. Khetprathum (2008) [10] studied concentration of protein from surimi by ultrafiltration, using pore-size membrane of 30 kDa and 100 kDa, pressure at 3.5 bar and cross-flow velocity of 360 L/h. The membrane rejection of protein was indicated about 98 %, and the protein concentration increased up to 10 %. The water permeated about 0.012 and the COD decreased from 30648 mg/L to 7684 mg/L.

1.2.2 Forward osmosis (FO)

Forward osmosis (FO) is one of the membrane-separation technologies for water reuse and desalination. The FO uses the different osmotic pressure from two side across a semi-permeable membrane. FO is the molecularity of water transporting across a selectively permeable membrane from low concentration to high concentration. The FO process can be applied for water distillation as well as another important applications such as food concentration, wastewater treatment, alcohol dehydration and power generation, etc. Table 1.2 shows the comparison between FO and RO process. The advantage of FO is no hydraulic pressure used the osmotic pressure difference from natural in this process. The FO process consumes low energy and lower membrane fouling comparing with the hydraulic pressure like reverse osmosis (RO) [25-28]. In addition, Figure 1.3 shows the FO process that focuses on;

(1) Development of material membrane such as high hydrophilic, high rejection, lower membrane fouling, good chemical resistance and good mechanical strength.

(2) Selectivity of new draw solution for high osmotic pressure and easy recovery as draw solution in FO process.

(3) Application used in full scale system.

Table 1.2. Comparison between FO and RO process.

Membrane process	**Advantages**	**Disadvantages**
Forward osmosis (FO)	- Less membrane fouling - Low energy consumption	-Salt leakage -Low water flux
Reverse osmosis (RO)	-High pure water	- High energy cost - High membrane fouling

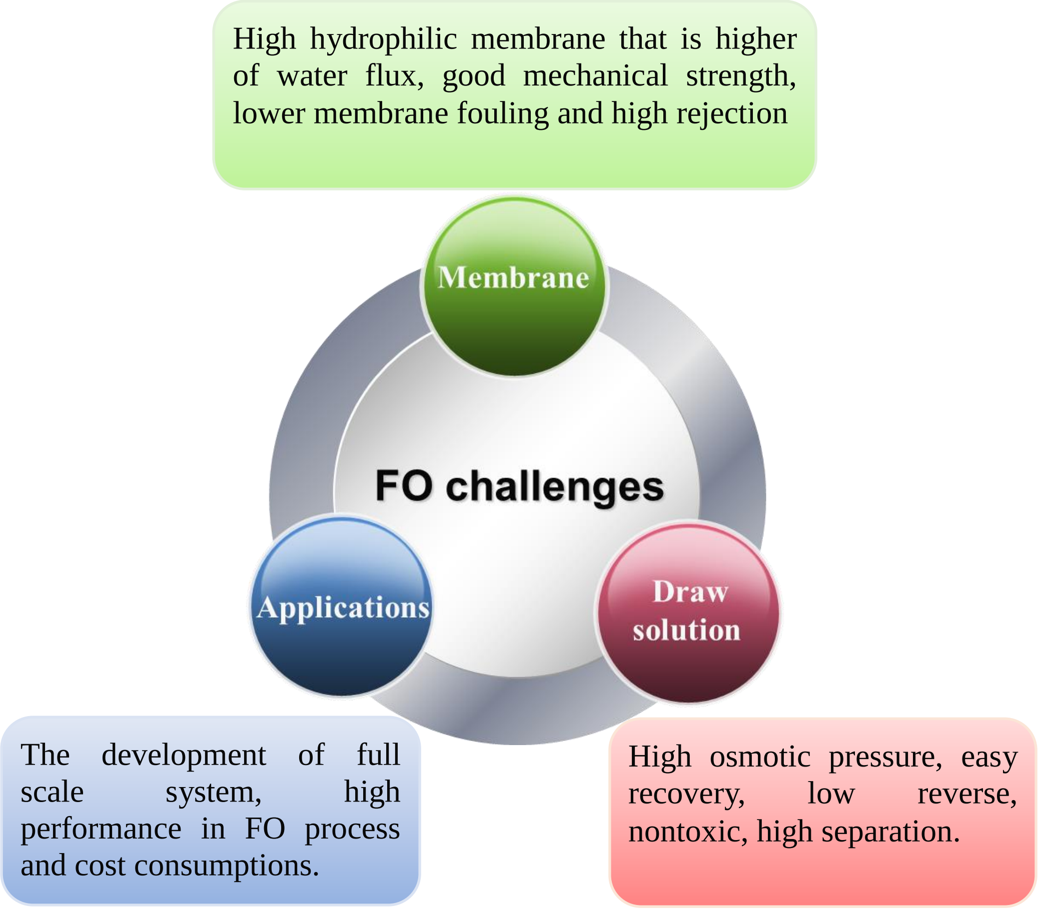

High hydrophilic membrane that is higher of water flux, good mechanical strength, lower membrane fouling and high rejection

The development of full scale system, high performance in FO process and cost consumptions.

High osmotic pressure, easy recovery, low reverse, nontoxic, high separation.

Figure1.2. The FO challenge process.

1.2.2.1 Principle of forward osmosis

Osmotic pressure driven in FO membrane process differs across concentration on semi-membrane from feed solution (FS) with the lower osmotic pressure in draw solution (DS) with higher osmotic pressure. Figure 1.3 shows the osmotic pressure maintained between lower concentration (equilibrium) classification of osmotic pressure in classification FO ($\Delta P = 0$), RO ($\Delta P>\Delta\pi$) and PRO ($\Delta P<\Delta\pi$). FO uses the osmotic pressure differential ($\Delta\pi$) across the membrane, rather than hydraulic pressure differential (as in RO), as the driving force for transporting the water though the membrane [37]. The osmotic pressure can be calculated by using Van’t Hoff’s equation

$$\pi = nCRT \tag{1.1}$$

Whereas,

π = osmotic pressure of a solution, kPa

n = the number of ions dissociated of one salt molecule

C = concentration, M

R = universal gas constant, 8.314 kPa.mol^{-1}.K^{-1}

T = temperature, K.

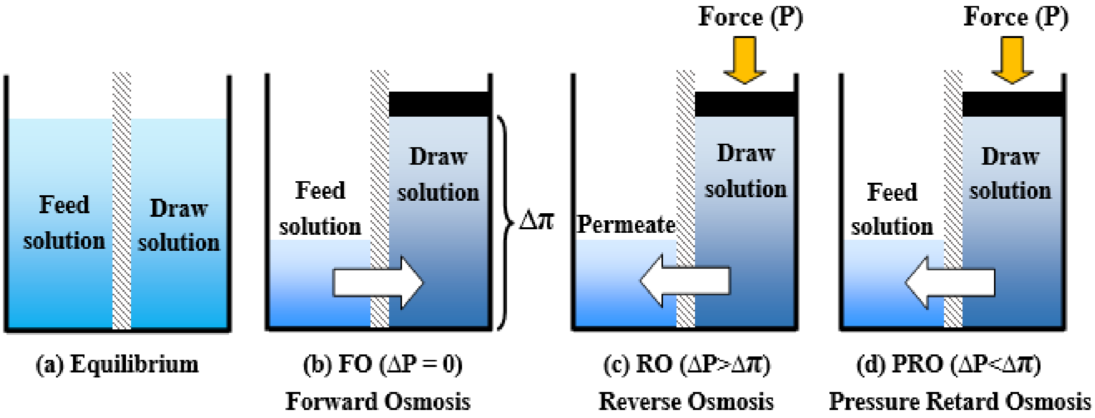

(a) Equilibrium **(b) FO ($\Delta P = 0$) Forward Osmosis** **(c) RO ($\Delta P > \Delta\pi$) Reverse Osmosis** **(d) PRO ($\Delta P < \Delta\pi$) Pressure Retard Osmosis**

Figure1.3. Classification of Osmotic Pressure (a) Equilibrium (b) FO ($\Delta P = 0$) (c) RO ($\Delta P > \Delta\pi$) and (d) PRO ($\Delta P < \Delta\pi$)

The general equation of water transport in an osmotically driven process is:

$$J_W = A\,(\Delta\pi - \Delta P) \tag{1.2}$$

A = water permeability coefficient (LMH)

$\Delta\pi$ = Osmotic pressure (bar)

ΔP = pressure (bar)

Where the water flux (J_W) can be expressed by the general equation used in FO

The water flux (Jw) in FO process can be expressed by the following equation;

$$Jw = A(\pi_{D,b} - \pi_{F,b}) \quad (1.3)$$

Where

A = water permeability coefficient (LMH)

$\pi_{D,b}$ = The osmotic pressure of draw solution

$\pi_{F,b}$ = The osmotic pressure of feed solution

1.2.2.2 Properties of FO membrane

FO membrane is the development of material challenges for improving the high water flux, low membrane fouling from feed solution (ECP) and draw solution (ICP), high rejection, good mechanical strength, and chemical resistance. The methods for preparing FO membrane include fabrication phase inversion and interfacial polymerization (IP) process. The FO membrane is a hydrophilic surface of any dense non-porous membrane. Table1.3 shows the report of development of FO membrane. The commercial of CTA-FO membrane was developed and marketed for a first time in the 1990s by Hydration Technology Inc. (HTI, Anllany OR). There are many types of material polymer of FO membrane such as cellulose acetate (CA), cellulose triacetate (CTA), Polybenzimidazole (PBI), polysulfone (PSF) and polyvinylpyrrolidone (PVP), polyamide and cellulose acetate etc [28-30]. The characterization of FO membrane is indicated below;

Table 1.3. Summary development of FO membrane

Year	Membranes	Materials	Preparation methods	References
2007	Hollow fiber NF	Polybenzimidazole (PBI)	Dry-jet wet phase inversion	[31]
2008	Flat sheet cellulose acetate	Cellulose acetate	Phase inversion and then annealing at 80–95 °C	[32]
2009	Dual-layer hollow fiber NF	PBI–PES/PVP	Dry-jet wet phase inversion (i.e. coextrusion technology)	[33]
2010	Hollow fiber	PES substrates, polyamide (PA) active layer	Dry-jet wet spinning and IP	[34]
2010	Hollow fiber NF	Cellulose acetate	Dry-jet wet spinning	[35]
2010	Flat sheet TFC	Polysulfone (PSf) support, PA active layer	Phase inversion IP	[36]
2011	Nanoporous PES	PES cast on PET fabric	Phase inversion	[37]
2011	Flat sheet TFC PA	PSf nanofiber support, PA active layer	Electro-spinning and interfacial polymerization	[38]
2012	TFC PA	Super porous CNT non-woven Bucky-paper (BP) support, PA active layer	Plasma treatment of CNT BPs support and IP	[39]
2012	Dual layer hollow fiber NF	PES inner support layer and PAI active layer post-treated by PEI	Dry-jet wet spinning, one-step coextrusion, multi-layer polyelectrolyte depositions	[40]
2013	Thin-film inorganic (TFI)	Stainless steel mesh (SSM) substrate, micro-porous silica xerogels active layer	Dip-coating and calcining for 4 h at 500 °C in nitrogen followed by cooling to 25 °C	[41]
2014	Thin-film nanocomposite (TFN)	PSf-titanium dioxide(TiO_2) nanocomposite substrate, PA active layer	IP	[19]
2014	Tri-bore hollow fiber TFC	Matrimid® 5218 polymer substrate, PA active layer	Dry-jet wet spinning and IP	[42]
2015	Flat sheet TFC	PEG celluloseester substrate,	phase inversion and IP	[43]
2015	Flat sheet TFC PA	polyamide active layer	Phase inversion and IP	[44]

1.2.2.2.1 Flat sheet of FO membrane

The flat sheet material of cellulose triacetate (CTA) is almost widely used for the first research in FO membrane process. These characterizations of CTA membrane are a hydrophilic membrane, salt rejection about 88 - 95 % and having water permeability of 2.1-3.8 LMH. The advantages of CTA membrane include a high hydrophilic of membrane which is higher of water flux, good mechanical strength and lower membrane fouling. The property of flat sheet FO membrane made of cellulose triacetate (CTA) has a polyester mesh embedded the material for mechanical support. The thickness of the membrane is less than 50 µm [29]. A SEM image cross-section and membrane surface of CTA-FO membrane SEM image of the commercial CTA-FO membrane clearly display in Figure 1.8.

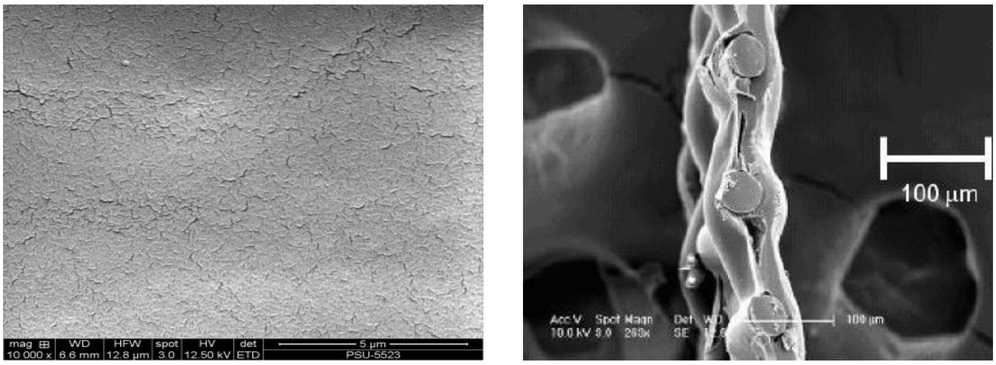

Figure 1.5. SEM image of cellulose triacetate (CTA) membrane,
(a) surface membrane (b) cross-section membrane [29].

1.2.2.2.2 Hollow fiber of FO membrane

The hollow fiber of FO membrane is the fabricated material of cellulose triacetate (CA). In other words, the cellulose triacetate nanofiltration (NF) hollow fiber is the material fabricated for FO membrane process. The material for hollow fiber of FO membrane is a hydrophilic of membrane. Figure 1.9 shows the contact angle 43˚of hydrophilic of membrane surface. The hollow fiber of FO membrane has the pore size of 0.3-0.63 nm. The water permeability characterization of hollow fiber of FO membrane is 1.34 LMH, and the salt rejection is 97 - 99 % [45].

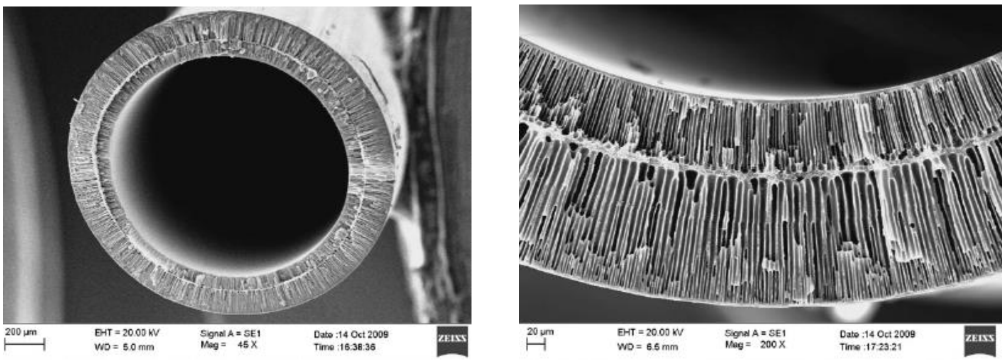

Figure.1.6 SEM image cross section hollow fiber membrane [45].

1.2.2.2.3 Thin film composite (TFC) of FO membrane

Thin film composite (TFC) of FO membrane needs to be further studied and used in FO and RO processes. These membranes must fabricate the material by using phase-inversion technique following interfacial polymerization (IP) of flat sheet membrane and hollow fiber membrane. Figure 1.7 shows the characterisation of TFC-FO membrane with a selective layer pore-size of 0.42 nm, and the salt rejection is 95 - 99.6 %. The substrate of membrane is made from polyethersulfone (PES), polyamide (PA), polysulfone (PS) and cellulose ester. The almost reports fabricated of polyamide is a selective layer and support layer made from polysulfone. The advantages of TFC-FO membrane include a high water flux and salt rejection [36, 39, 43, 44].

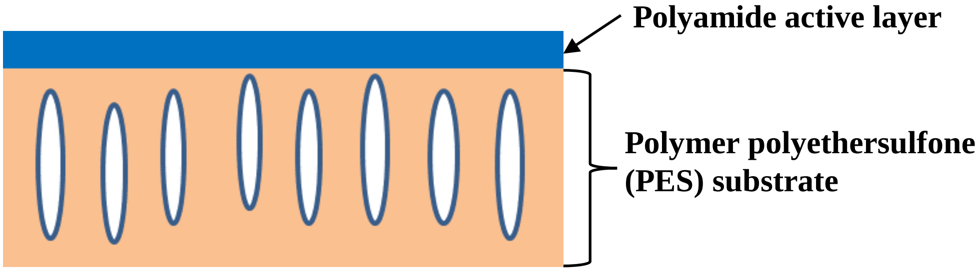

Figure 1.7. The characterization of TFC membrane [43].

1.2.2.2.4 Thin film nanoparticle (TFN) of FO membrane

Recently, the new type of material membrane is the thin film nanoparticles (TFN). Figure 1.8 shows that these membranes are prepared via IP in process and made from polyamind (PA) on selective layer while the support layer is made from of material polymer such as polysulfone (PS) or polyethersulfone (PES) and mixed matrix such as zeolite NaA nanoparticle or titanium dioxide (TiO_2). The characterisation of TFN membrane has a pore size of 0.74-0.79 nm, the high salt rejection of 97.4 - 98.7 % and the water permeability of 4.2×10^{-12} m Pa^{-1} s^{-1} [19, 46, 47].

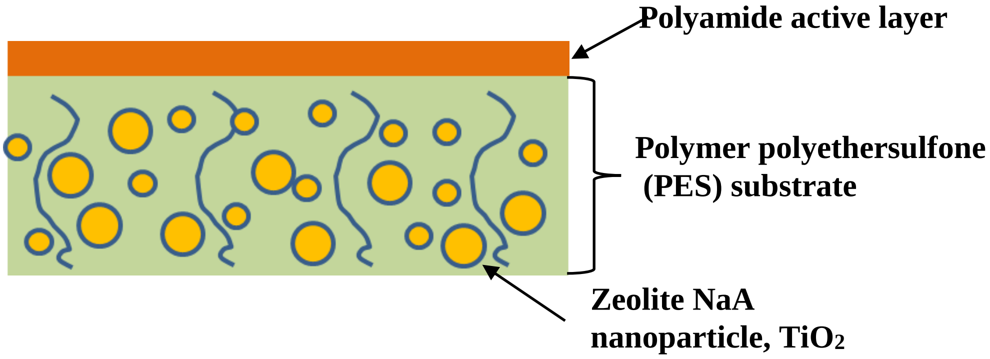

Figure.1.8 The characterization of TFN membrane [46].

1.2.2.3 The operating conditions in FO process

1.2.2.3.1 Concentration

The concentration of draw solution in osmotic driven water from high concentration is to lower concentration across semi-permeable in FO processes. The high concentration is a greater osmotic pressure which can increase the water flux [48].

Table 1.4. Summary of commercial of membrane, application, operating condition and flux commonly use in FO processes

Operation temp (°C)	**Feed**	**Draw solution**	**Draw flow rate**	**Membranes**	**Water flux (LMH)**	**Reference**
23 ± 1.0	DI water	1.0 M NaCl	1.5 L/min	CTA flat sheet membrane A, HTI.	16.8	[16]
23 ± 1.0	DI water	1.0 M NaCl	1.5 L/min	CTA flat sheet membrane B, HTI.	12.4	[16]
23 ± 1.0	DI water	1.0 M NaCl	1.5 L/min	CTA flat sheet membrane C, HTI.	6.6	[16]
20 ± 1.0	50 mM NaCl	4.0 M NaCl	0.085 cm/s	CTA flat sheet membrane, HTI.	27	[49]
23 ± 0.5	DI water	5.0 M MgCl2	0.73 m/s	Dual-layer (PBI-PES/PVP) NF hollow fiber membrane	24.2	[50]
20 ± 2	DI water	1.5 M MgSO4	5.5 L/min	TS80 NF TFC membrane, TriSep	11	[51]
25 ± 0.5	DI water	1.5 M NaCl	0.21 m/s	TFC polyamide flat sheet membrane	18	[52]
20 ± 1.0	sucrose	2 M NaCl	21.4 cm/s	CA Flat sheet, HTI	9	[53]
30 ± 1.0	sucrose	2 M NaCl	21.4 cm/s	CA Flat sheet, HTI	17.22	[53]
20 ± 1.0	sucrose	4 M NaCl	21.4 cm/s	CA Flat sheet, HTI	18.11	[53]
30 ± 1.0	sucrose	4 M NaCl	21.4/ cm/s	CA Flat sheet, HTI	23.88	[54]
21.0 ± 1.0	BSA	5.0M NaCl	8.5 cm/s	CTA Flat-sheet, HTI	25.2	[55]
25 ± 1.0	Oil&gas waste	NaCl 50g/L	1 L/min	CTA Flat-sheet, HTI	10	[56]

1.2.2.3.2 Cross-flow velocity

The operation condition with the cross-low velocity could increase the water flux presented in Table 1.4. The feed or draw solution feed high flow rate can improve the water transmembrane flux and decrease the fouling because the hydrodynamic shear force may increase with increasing feed flow rate. In addition, the feed of mode in co-current and counter-current flow could be improve the water flux and reduce the concentration polarization on membrane surface [28].

1.2.2.3.3 Temperature

The temperature plays a significant role in the FO process as temperature has direct influence on the thermodynamic properties of both the draw solution (DS) and the feed solution (FS). The FO permeation of flux has been observed about 12.3 %, and it is up to 45.4 % when the temperature of the FS and DS increases to 35 °C and 45 °C. Phuntsho et al,. (2012) [57] studied the effect of working temperature on separation performance and found that when the feed solution in FO reached the temperature of 25, 35 and 45 Ċ, it marked that higher temperature would afford higher initial flux, higher water recovery and higher concentration factors. Table 1.5 shows the difference of temperature in FO process.

Table 1.5. Summary of Difference of Temperature research in FO process.

Temperature	Feed solution	Draw solution	Flow rate (cm/s)	Membrane	Flux (LMH)	Reference
20 ± 1.0	sucrose	2 M NaCl	21.4	CA Flat sheet, HTI	9	[53]
30 ± 1.0	sucrose	2 M NaCl	21.4	CA Flat sheet, HTI	17.22	[53]
20 ± 1.0	sucrose	4 M NaCl	21.4	CA Flat sheet, HTI	18.11	[53]
30 ± 1.0	sucrose	4 M NaCl	21.4	CA Flat sheet, HTI	23.88	[53]
25 ± 2.0	Brackish	1.5 M Na_2SO_4	25	CA Flat sheet, HTI	15.13	[32]
35 ± 2.0	Brackish	1.5 M Na_2SO_4	25	CA Flat sheet, HTI	19.79	[32]
45 ± 2.0	Brackish	1.5 M Na_2SO_4	25	CA Flat sheet, HTI	22.09	[32]
25 ± 0.5	Salinity	117 g/L NaCl	10	CA Flat sheet, HTI	14	[59]
35 ± 0.5	Salinity	118 g/L NaCl	10	CA Flat sheet, HTI	19	[59]
45 ± 0.5	Salinity	119 g/L NaCl	10	CA Flat sheet, HTI	23	[59]

1.2.2.4 Membrane fouling in FO process

1.2.2.4.1 Internal concentration polarization (ICP)

One of the major factors in limiting the water flux in osmotic driven membrane process is the severe internal concentration polarization (ICP). This phenomena occurs in the porous support layer of membrane as presented in Figure 1.9 (a).

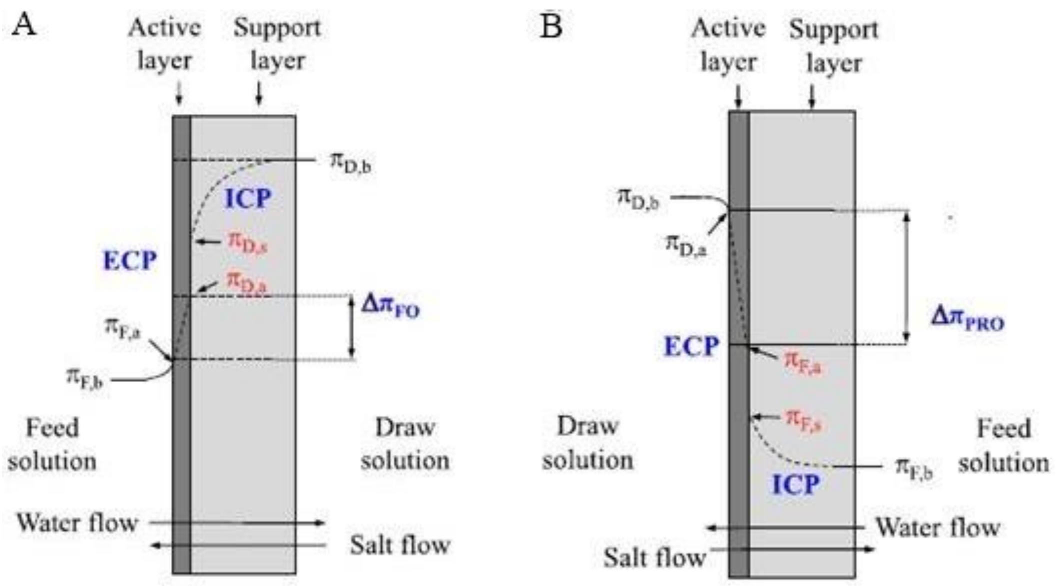

Figure 1.9. Show FO membrane transport modeling (a) ICP (b). ECP [38].

1.2.2.4.2 External concentration polarization (ECP)

The second term of concentration of feed solution and draw solution is the external concentration polarization (ECP). The ECP occurs on the external surface of the selective layer from draw solution (DS) while the feed solution (FS) flows against the porous support layer shown in Figure 1.9 (b) [38].

1.2.2.5 Draw solution in FO process

The draw solution in FO process is a selection for influencing properties which make high osmotic pressures, easy separation from water, lower solute reverse, low viscosity, nontoxic and economic feasibility. However, the main problem of draw solution is a salt leakage. It contaminates the product. In addition, numerous types of draw solution used in FO processed have been researched. For example, NaCl is used as the standard in many FO-process researches. There are several types of draw solution such as $MgCl_2$, KNO_3 $MgSO_4$, sucrose, mixing ammonium bicarbonate (NH_4HCO_3) ammonium hydroxide (NH_4OH) etc. Recently, some types of draw solution have been developed to provide high osmotic pressure in order to enhance the water flux comparing with the NaCl standard presented in Figure 1.10.

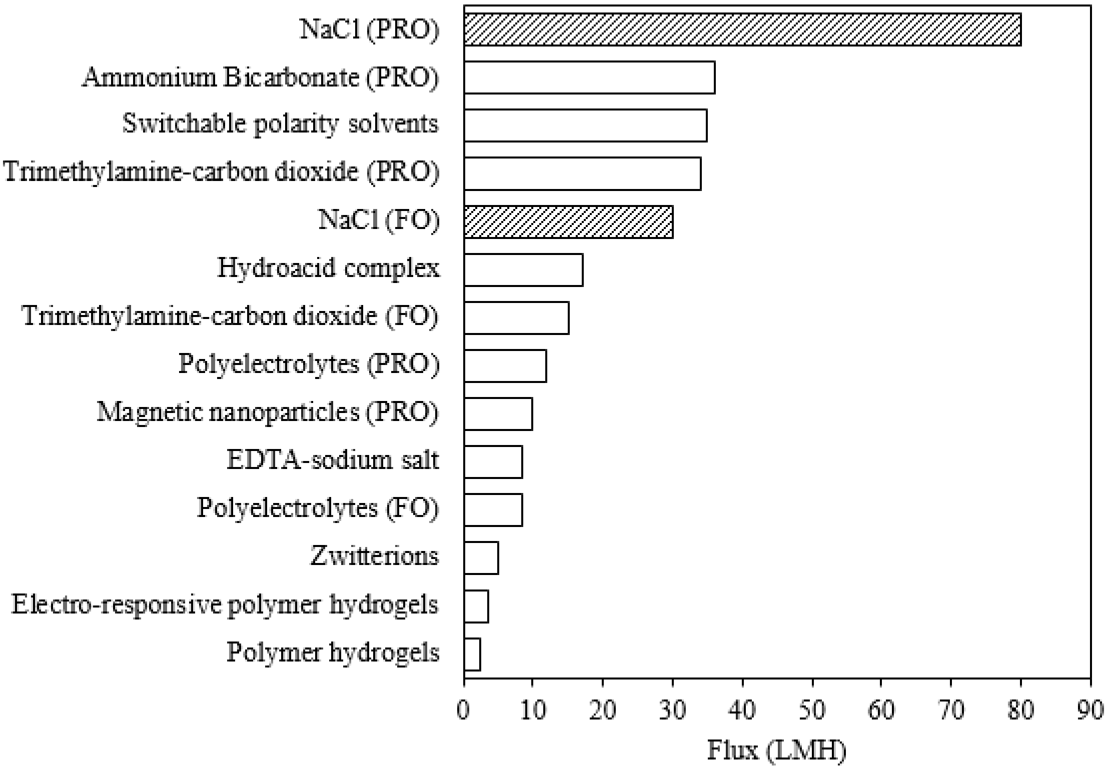

Figure1.10. The develop type of draw solution comparison with NaCl standard in FO process [60].

1.2.2.6 Draw-solution recovery process

The draw-solution recovery process is for recovering the concentration from dilute as draw solution for constant concentration technology in FO process. Numerous technologies have been continuously researched and developed for recovery the draw solution. Table 1.6 shows types of draw-solution development and recovery approaches in FO technology. Most researches of water recycle of hybrid system that used FO/MD, FO/UF, FO/NF and FO/RO succeeded to produce the clean water [48, 60, 61].

Table 1.6. The methods of recovery as draw solution

Year	**Draw solute/solution**	**Recovery methods**	**Reference**
1992	Sugar	RO	[62]
2002	KNO_3 and SO_2	SO_2 is recycled through standard mean	[63]
2005-2007	NH3 and CO2 (NH4 HCO3)	Moderate heating (~60Ċ)	[64
2007	Dendrimers	Captured by a canister sepator	[65]
2010	2-Methylimidazole-based solutes	Denatured and solidified by heating	[66]
2010-2011	Magnetic nanoparticles	MD	[67]
2011	Hydrophilic nanoparticles	UF	[68]
2012	Polyelectrolytes	UF	[69]
2012	Hydrophilic nanoparticles	NF	[70]
2012	Organicsalts	RO	[71]
2012	polyglycolco polymers	NF	[72]
2013	Thermo-sensitive polyelectrolyte	UF	[73]
2013	Copper sulfate	Metathesis precipitation	[74]
2013	Magnesium sulfate	Metathesis precipitation	[75]
2014	Hydroacid complexes	NF	[76]
2015	Electric-responsive polymer hydrogels	Electric field	[77]
2015	PAMAM-COONa	MD	[78]
2015	Thermo-responsive microgels	Centrifugation at 40	[79]
2015	Poly (sodium 4-styrenesulfonate)	UF	[80]

1.2.2.6.1 The hybrids FO/UF, FO/NF and FO/RO process

The hybrid technology for recovery the recycling concentration as the draw solution and freshwater product. Figure 1.11 shows the recent membrane processes such as UF, NF and RO which are widely used in membrane technology process.

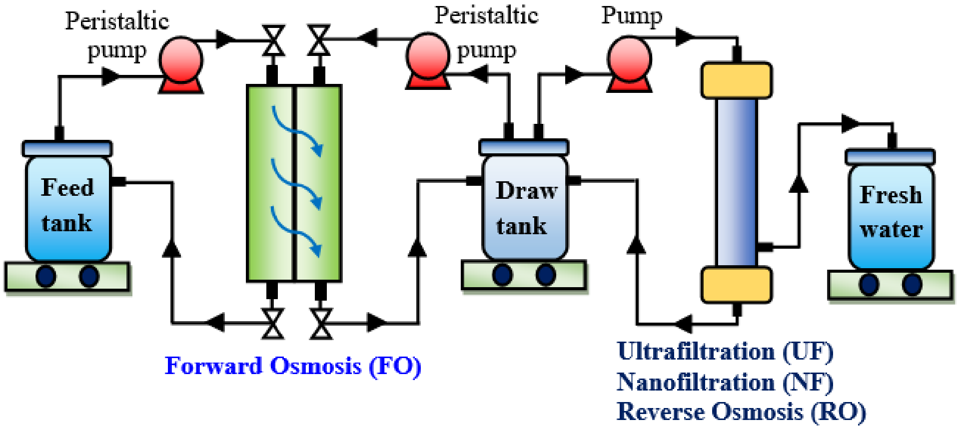

Figure 1.11. Hybrids of FO/UF, FO/NF and FO/RO process [69].

1.2.2.6.1.1 Forward osmosis/Ultrafiltration (FO/UF)

UF membrane can separate the molecular weight range of 0.2-0.02 micro. UF membrane operates with the hybrid system in FO process for recovery the draw solution and clean water. Ge at al,. (2012) [68] earlier studied the use of FO/UF process for recycling PAA-Na solutions as the draw solution. The hybrid of the process used cross-flow velocity of 6.4 cm/s, the PAA-Na MWCO 1200, 1800 and 5000 Da as the draw solution. The FO/UF process specified that the UF membrane rejection more than 98.5% of PAA-Na (1200), higher rejection >99% of PAA-Na (1800, 5000) and recycling up to five times.

1.2.2.6.1.2 Forward osmosis/Nanofiltration (FO/NF)

In hybrid of FO/NF system, the NF membrane can be applied in hybrid in FO process for recovery as the draw solution. The NF membrane filtration of MWCO rang is 100-1000 Da, and it uses the pressure rang at 5-10 bar. The NF membrane's advantages include a high rejection rate, lower operating pressure and low maintenance cost over RO processed. Tan et al,. (2012) [81] studied the desalination from sea water and recovery the draw solution in hybrids of FO/NF. It was found 97 % that recovery the concentration is used as the draw solution. TDS decreased at 113.6 mg/L. Zhao et al,. (2012) [55] studied the desalination from sea water by using hybrids of FO/NF system, polyamide TFC membrane and feed solution Na_2SO_2 as draw solution. The cross-flow velocity was 25 cm/s, NF membrane used pressure at 4.8 bar. It was also found that this recovery process of concentration as draw solution is 90 %. In addition, continuing the process can make the lower membrane fouling and higher flux, comparing with RO process. Kumar and Pal (2015) [82] studied the waste-water treatment and the recovery concentration as draw solution in hybrids of FO/NF system. The feed solution was 1.5 M as draw solution, cross-flow velocity at 42 cm/s and pressure in NF membrane at 10 bar. It was found that the water flux was 46 LMH, and the COD decreased. The recovery concentration as draw solution was 99 %, and the average of water flux was 45 LMH.

1.2.2.6.1.3 Forward osmosis/Reverse osmosis (FO/RO)

FO/RO processes is membrane separation method for recovering the draw solution in hybrids of FO process. RO membrane can be separated in the molecular weight of 100-1000 Da of rejection. The high mono-valent ion is 90-99 %, rejection high efficiency of divalent ion. The pressure used in RO processed is 10-100 bar. The advantages of FO/RO process include high water recovery rate and high salt rejection, but operating cost is still high [28].

1.2.2.6.2 Hybrids process FO/MD

FO/MD is a hybrids process for recovering the draw solution from dilute concentration and fresh water. Figure 1.12 shows the FO/MD using the different temperature, higher and lower temperature across semipermeable membrane. The process shows advantages of high water recovery, high water quality and lower capital cost, but operating cost is also high. [78].

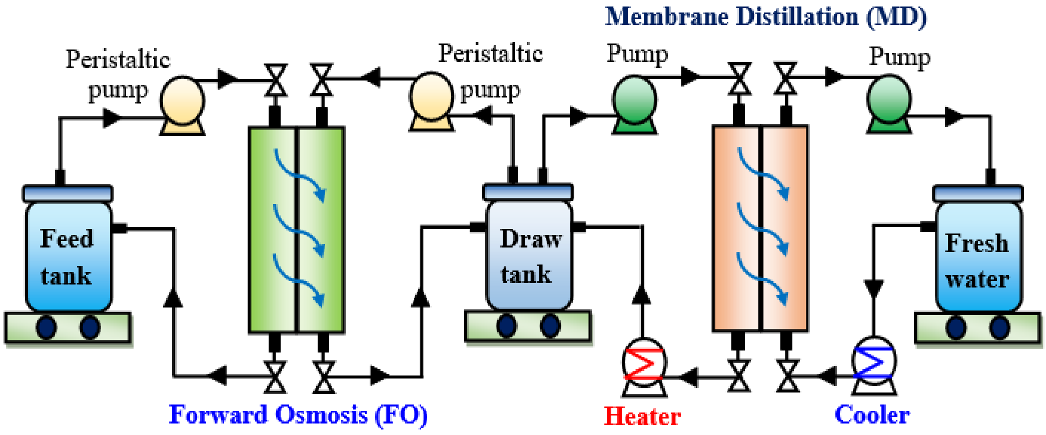

Figure 1.12. Hybrids of FO/MD process [78].

1.2.2.6.3 Magnetic field process

Figure 1.7. Indicates the magnetic field process, this process is used for regeneration of magnetic nanoparticles (MNPs) as draw solution. The advantages of this method include easy separation and high water recovery rate. However, the disadvantages also include poor agglomeration and poor water quality. Ge et al., (2012) [67] studied the regeneration of MNPs by using magnetic field. This separated agglomeration of MNPs, so the osmotic pressure decreased and lowered the water flux. However, the prevention of agglomeration of MNPs is to use ultrasonic technical, but reducing the regeneration form potentially weakens the MNPs. Ling et al,. (2011) [68] studied the separation of MNPs by using magnetic field. This made the easy separation, high regeneration efficiency and sly aggregation.

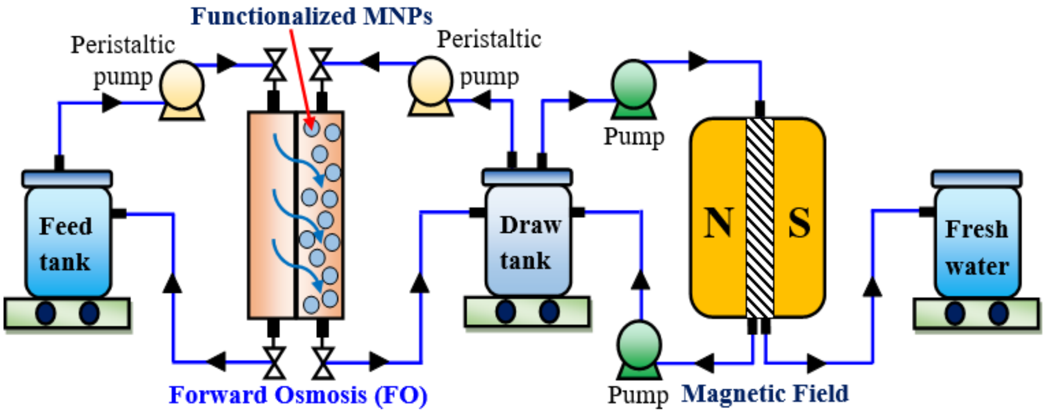

Figure 1.13. Hybrids of FO/Magnetic field process [66].

1.2.2.6.4 FO/heating

The hybrids of FO/heating system is also used for recovering the concentration by using low temperature. M.Ginnis et al,. (2002) [63] and M. cutcheon et al,. (2005) [64] studied the use of hybrids of FO/heating system for recovery and separation of NH_3/CO_2 as draw solution at 60 ºC. It was found that the concentration recovery of NH3/CO_2 is 64 % and is easily separated from draw solution. The hybrids of FO/Heating process is shown in Figure 1.14.

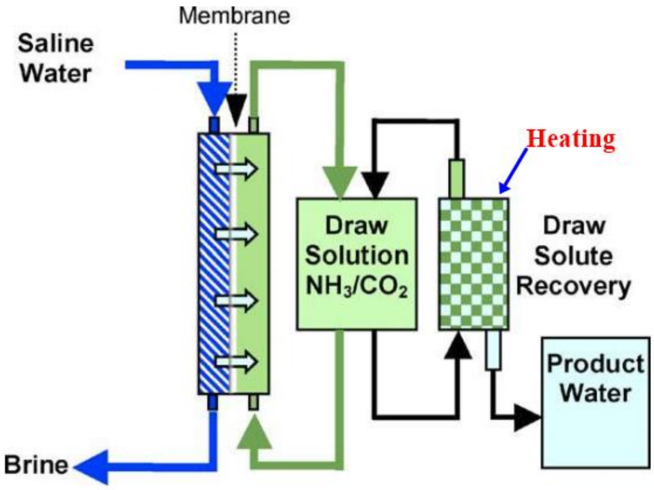

Figure 1.14. Hybrids of FO/Heating process [64].

1.2.3 Modification membrane surface

There are many methods to modify the membrane surface such as plasma treatment, UV irradiation, and graft polymerization. The plasma treatment is one of the most promising technologies for membrane modification such as cross-link chin of polymer, etching and absorption. Table 1.7 presents the plasma method for modification of membrane surface. Particularly, the grafting polymerization is considered a very effective approach to form the permanent surface of membrane hydrophilic. Modification of cellulose triacetate membrane (CTA) surface could improve to hydrophilic by gas plasma treatment [12, 83].

Table 1.7. Summary method modification membrane surface

Membrane process	Membrane	Polymer grafting	Power (w)	Gas treated	Reference
UF	poly(tetrafluoroethylene)	Acrylic acid	50	Ar	[84]
UF	Polyurethane	Acrylic acid	10-30	Ar	[85]
UF	PTFE	Acrylic acid	40-90	O_2	[86]
UF	PTFE	Polyacylic acid	40-90	Air,N_2	[86]
UF	poly ε-caprolactone	TiO2	35	O_2	[87]
UF	polyethersulfone	AAc	25-50	Ar	[88]
PV	Cellulose triacetate	-	47-49	CO_2	[89]
-	polyethersulfone (PES)	Acrylamide (AAm)	40	CO_2	[90]
RO	polyethersulfone (PES)	PEG	10	CO_2	[91]

Plasma treatment is a technique to modify membrane surface which can change the surface properties of the chain polymer such as amino and hydroxyl group (hydrophilic functional group). The methods of plasma are plasma treatment and plasma grafting polymerization. It is explained as follows;

1.2.3.1 Plasma treatment

By modifying the membrane surface with plasma treatment, the gas plasma such as O_2, Ar, CO_2 activated on substrate via the corresponding of the peroxide and hydroxyl group of more hydrophilic functional groups. The plasma treatment with gas plasma pointed out higher hydrophilic membrane and decreased membrane fouled of the protein, gelatin and alginate solution [92]. Modification of membrane surface by gas plasma treatment can also upgrade the properties of hydrophilic polymer and the bonding of hydrogen, essentially with water molecules to hydrophilic, C=O, C=N and OH of amino group. The mechanism of the plasma treatment is shown in Figure 1.15.

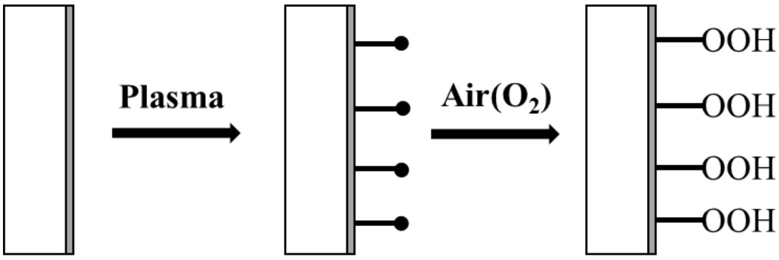

Figure 1.15. The mechanism of the plasma treatment [92].

Riekerink et al,. (2002) [89] studied the hydrophilic of cellulose triacetate of membrane surface. The gas plasma used CF_4 at plasma discharge of 47-90 W and pressure of 0.04-0.08 mbar at 0-15 min. It was found that the optimising time was 15 minutes, and the contact angel decreased from 66 ˚ to 0 ˚. For the XPS analysis, it was found that the O increased from 35.5 % up to 47.6 %. For the AFM analysis, it was found that the roughness increased and etched on membrane surface. Regarding the performance of membrane, the water flux eventually increased and membrane foulant decreased to 30 %.

Bhat and Wavhal (2002) [93] studied the modification of cellulose triacetate membrane in pervaporation (PA) by using gas ammonia (NH_3) of plasma discharge of 10 w at pressure 0.15 Torr. After modifying the membrane, it was found that the optimizing time was 5 min. The contact angle decreased from 59˚ to 43˚. For the FTIR analysis, it was found that the functional group –OH and C=O increased the concentration of hydrophilic and had excellent selectivity for water. For the SEM image analysis, the roughness also increased and etched on membrane surface. Regarding the performance of membrane, the water flux increased and membrane foulant decreased as well.

1.2.3.2 Plasma grafting polymerization

Modifying the membrane surface by grafting with hydrophilic monomer is a method that makes the hydrophilic monomer attached to the membrane surface. Its advantages involved the improvement to hydrophilicity membrane surface and antifouling membrane. The plasma grafting of monomer can be the formation of polymeric material. In addition, titanium dioxide (TiO_2) is the nanoparticle used for grafting on membrane surface and mixing the matrix membrane for increasing hydrophilic. TiO_2 also has its advantages that include high hydrophilic, mechanical strength and anti-bacteria. [87, 92].

Figure 1.16 shows the mechanism of the plasma grafting polymerization (lower molecular weight). The first step, the gas plasma was activated on the surface substrate. After the plasma activated membrane was exposed to air or oxygen, the peroxide group was formed. This formation of peroxide group is made the substrate ready to graft the AAc monomer. Lastly, the hydroxyl group was generated on the substrate [92].

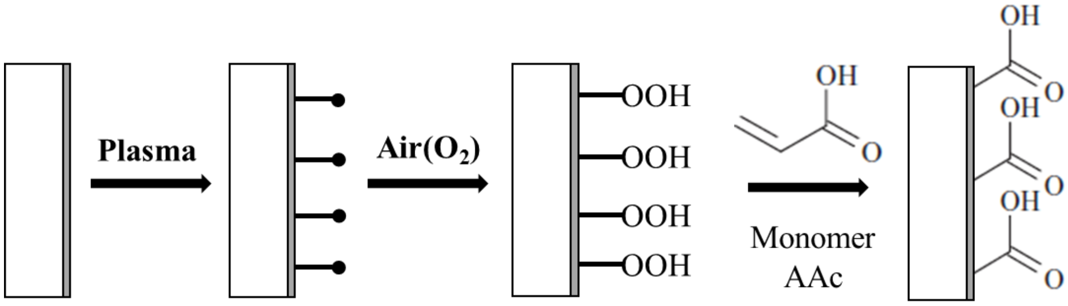

Figure 1.16 the mechanism of the plasma grafting polymerization [91].

Weibel et al,. (2007) [85] studied the hydrophilic of membrane surface in pervaporation by using O_2 and N_2 gas plasma grafting AAc on polyurethane (PU). The plasma discharged of 13.56 MHz at pressure at 8-30 Pa. membranes. It was found that the contact angle decreased from 81˚ to 41 ˚ and 52 ˚ for plasma gas O_2 and N_2, respectively. For the XPS analysis, the functional group of C-C was increase to the COO and C=O function group after AAc grafting polymerization. Zao et al (2011) [91] studied hydrophilic of TFC membrane surface by using the plasma PEG grafting polymerization at the plasma discharge of 1 w during the time of 10-20 s. After the modification, the contact angle decreased from 32˚ to 7 ˚ at 120 minutes. The membrane foulant decreased to 27 %, and after membranes cleaning, the water flux was up to 99.5 %. Tores et al,. (2014) [94] studied the hydrophilic of cellulose acetate of plasma poly (acrylic) acid (PAAc) by using the grafting polymerization of membrane surface. O_2 is used with the plasma discharge of 1-2 kW at 1-10 min. After the modification, it was found that the contact angle decreased from 120 ˚ to 60.3 ˚ at plasma discharge of 1 kW at only 1 minute. For the XPS analysis, the functional group of carboxyl (-COOH) increased after modifying membrane. Moghnimifar et al,. (2014) [95] studied hydrophilic of polyethersulfone (PES) in ultrafiltration membrane by using plasma corona gas and plasma TiO_2 grafting polymerization at plasma discharge 180-360 w, during the time of 2-6 minutes. After modifying the membrane, it was found that the contact angle of M19 membrane decreased from 65˚ to 0 ˚. For the AFM analysis, roughness also increased from 25.3 nm to 34.7 nm. For the FTIR-ATR analysis, the functional group increased the COOH. Regarding the performance, the water flux was 17 LMH and stayed constant. The membrane separation of oil was 99 %.

1.3 Objectives

The objectives of the study are as follows;

1. To modify the membrane surface by using plasma treatment for enhancing the flux and salt leakage
3. To study the effect of operation condition on water flux and salt leakage in FO process.
2. To recover the protein concentration from tuna cooking juice.

The scope of this work is presented in Figure. 1.17.

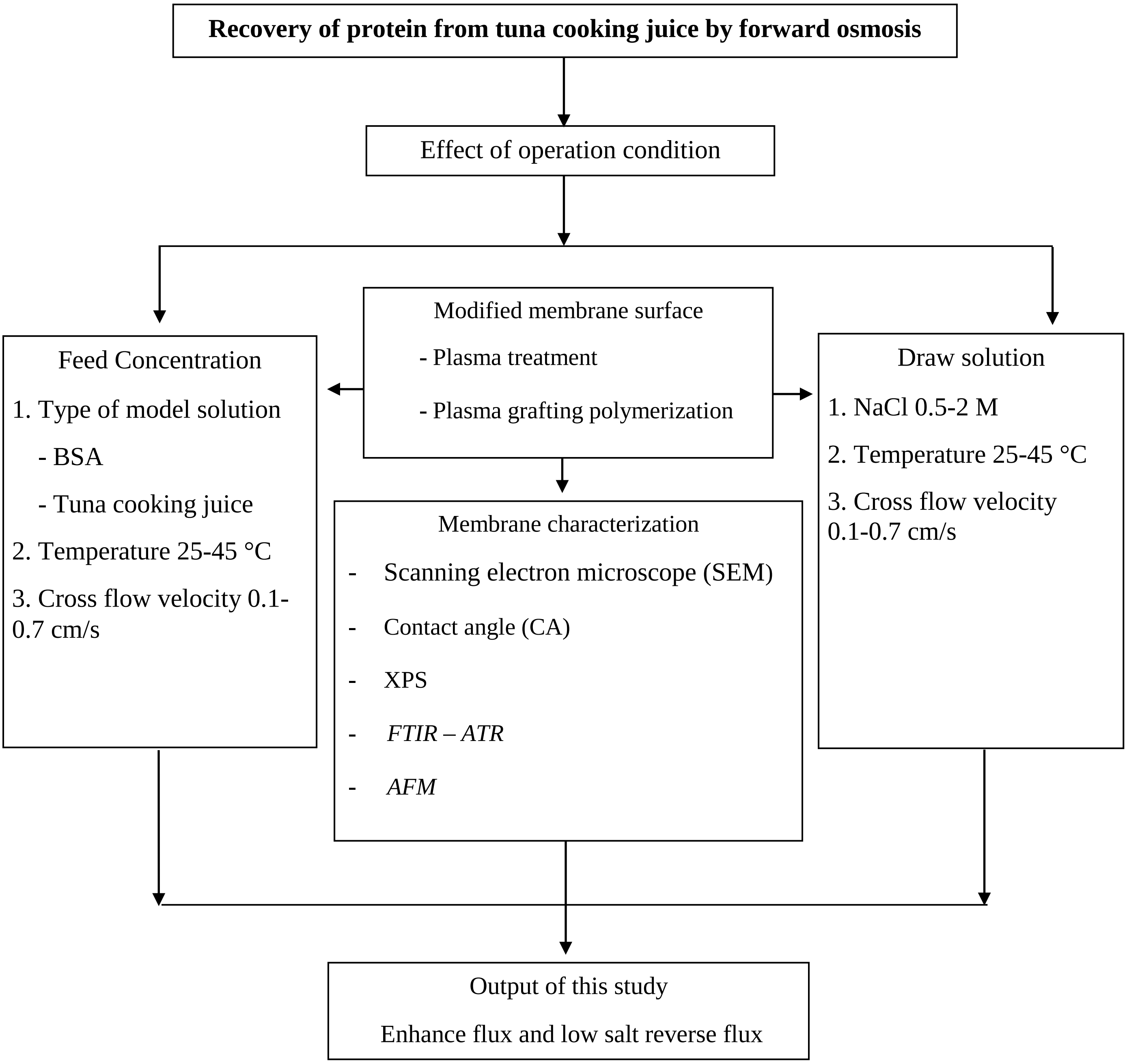

Figure 1.17. Scope of work in this study.

Chapter 2

Material and methods

2.1 Material

The commercial cellulose triacetate (CTA) membrane was purchase from Hydration Technology Innovations (HTI, Abalny, OR, USA).

The bovine serum albumin (BSA, purity 98%, MW 66 kDa), titanium dioxide (purity 99 %, MW 79.90 g/mol) and Acrylic acid (AAc, purity 99%, 200 ppm) were purchased from Loba Chemie, Mumbai, India. Sodium chloride (NaCl, purity 99.9 %) was purchase from Ajax Finechem. Sodium hydroxyl (NaOH, purity 99.9 %) was purchase from Merck KGaA, Germany.

Tuna cooking juice was obtained from Tropical Caning (Thailand) Public Company Limited, Hat Yai, Thailand.

2.2 Methods

2.2.1 Modification of membrane surface

2.2.1.1 Plasma treatment

The DC glow discharge plasma reactor was generated in the vacuum chamber consisting of 25.4 cm internal diameter and 38.1 cm length as shown in [96] Figure 2.4. The base pressure within the reactor was typically in the range of 5.0×10^{-4} mbar. The CO_2 plasma flow was adjusted to obtain a steady pressure at 0.4 mbar and to create the plasma power by a needle valve. The plasma power was varied in the range of 10-50 watts and the exposure time was employed at 5, 10, 15, 20 and 25 min, respectively. The optimize of CO_2 and Ar gas plasma treatment were compared and selected with the parameter in Table 2.1 Ar gas plasma treatment.

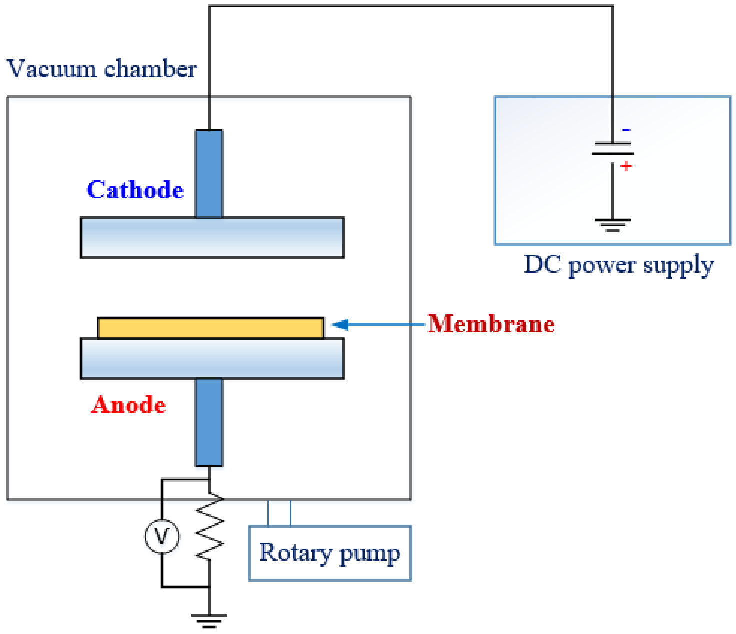

Figure 2.1. The diaphragms of DC plasma discharge [96].

2.2.1.2 Plasma AAc and TiO_2 grafting polymerization

The CTA membrane samples (7 cm x 14 cm) were prepared and taped on a glass. The plasma gas treated with ambient to the air for 30 min. Each Ar gas plasma flow was adjusted to get a steady pressure of 0.25 mbar. The power discharge at 20 watts for the duration between 5-20 seconds. After treatment, CTA membrane was quickly immersed in solution with contained 10 % (w/v) AAc solution for 30 min in water bath. The water bath temperature maintain at 40 °C. After that, it was rinsed the reside monomer with DI water. Then, the sample wasat 40 °C for 30 min.

Plasma modification and coating of TiO_2 on surface were employed following Moghimifar et al,. (2014) [95]. The CTA membrane samples (7 cm x 14 cm) were prepared and taped on a glass. The plasma gas treated with ambient to the air for 30 min. Each Ar and CO_2 gas plasma flow was adjusted to get a steady pressure of 0.25 mbar. The power discharge at 20 watts for the duration between 5-20 s. After treatment CTA membrane was quickly immersed in solution with contained 1 % (w/v) of TiO_2 concentration for 30 min in ultrasonic bath. Then, the samples were dried at 40 °C for 30 min.

2.2.2 Characterization membrane

2.2.2.1 Physical analysis

The morphology of CTA membrane was characterized by scanning electron microscope (SEM-Quanta, FEI Quanta 400). The hydrophilicity of membrane surface was determined by water contact angle (Data Physics Instruments OCA15 GmbH, Filderstadt, Germany). The water droplet with volume of 1μL/s was formed on the membrane surface. Each measurement was tested in triplicate and their average value were calculated [12].

2.2.2.2 Chemical analysis

The chemical component of membrane surface was analyzed by X-ray photoelectron spectroscopy (XPS, AXIS Ultra DLD, Krotos, Analytical Ltd. UK). The surface chemical structures of CTA membrane and plasma treatment CTA membranes were analyzed by Attenuated Total Reflectance- Fourier transform Infrared spectroscopy, ATR-FTIR (Tensor 27, Bruker, US). The surface roughness was measured by atomic Force Microscope (AFM, NanosurfeasyScan2). The summary of method for measurement the membrane properties presented in Table 2.1

Table 2.1. The method of measurement of membrane properties

Measurement	Technique for
Contact angle (CA)	The hydrophilic of membrane surface
Fourier transform Infrared spectroscopy (FTIR-ATR)	Chemical surface functional group
Scanning electron microscope (SEM)	Morphology of surface
Atomic Force Microscope (AFM)	Morphology of roughness
X-ray photoelectron spectroscopy (XPS)	High resolution chemical functional group

2.2.3 Performance of membrane

2.2.3.1 Water permeability coefficient

The performance of CTA membrane was characterized by measuring the water permeability coefficients of pure water flux and salt rejection. The water permeability coefficient (A; LMH.bar^{-1}) and salt rejection (R; %) were tested with RO mode Figure 2.2. Deionized (DI) water was supplied as feed solution at the applied pressure between 1-5 bars. DI water was used as feed solution for water permeates flux testing. The water flux (J_w) was calculated as follows:

$$Jw = \frac{\Delta\ weight}{water\ density \times effective\ membrane\ area \times \Delta\ time} \qquad (2.1)$$

2.2.3.2 Salt permeability coefficient

The salt permeability coefficient (B; LMH) was calculated as follows:

$$\mathrm{R} = 1 + \left(\frac{(B)}{A(\Delta p - \Delta\pi)}\right)^{-1} \qquad (2.2)$$

Whereas, A is water permeability coefficient (LMH.bar^{-1}), ΔP (bar) the difference pressure across membrane and Δπ (bar) is the osmotic pressure across membrane

2.2.3.3 Salt rejection

The salt rejection testing used 10 mM of NaCl for feed solution. The salt rejection was calculated as follows:

$$R = (1 - \frac{Cp}{Cf}) \times 100 \qquad (2.3)$$

Whereas Cp and C_f are the salt concentration of permeate solution and feed solution, respectively.

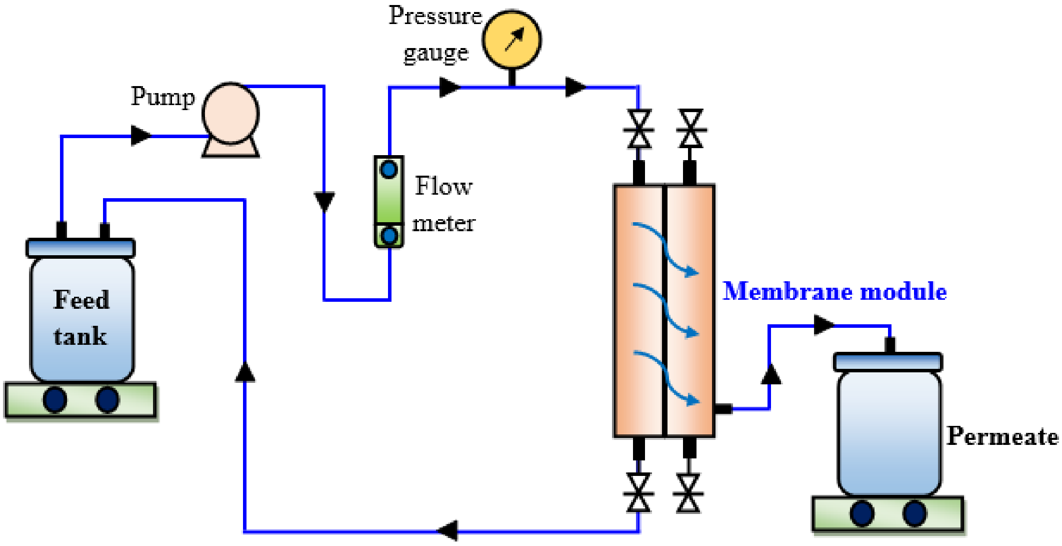

Figure 2.2. The RO test unit

2.2.4 Operating condition in FO processes

2.2.4.1 The FO system

The FO experiment was set up as shown in Figure 2.3 and Figure 2.4 the membrane unit was presented which consisted of 20 cm long, 10 cm wide, and 0.3 cm depth on both permeate and feed sides of membrane. The water flux was analyzed with DI water at 0.10 cm/s in the feed side. The draw solution flow was conducted in co-current mode with the velocity at 0.70 cm/s by peristaltic pump (EYELA MP-3N, Japan). The pressure monitoring was measured by the pressure transducer (TR-PS2W-2bar Lutron, Taiwan) in both FS and DS.

BSA of 1 gL^{-1} as feed solution (FS) and 2 M NaCl was used for draw solution (DS). The concentration of NaCl measured by conductivity meter (WTW MF318, Germany).The weight of permeate was measured by digital balance (AND GF-3000, Japan) and collected the data by direct connect to the computer.

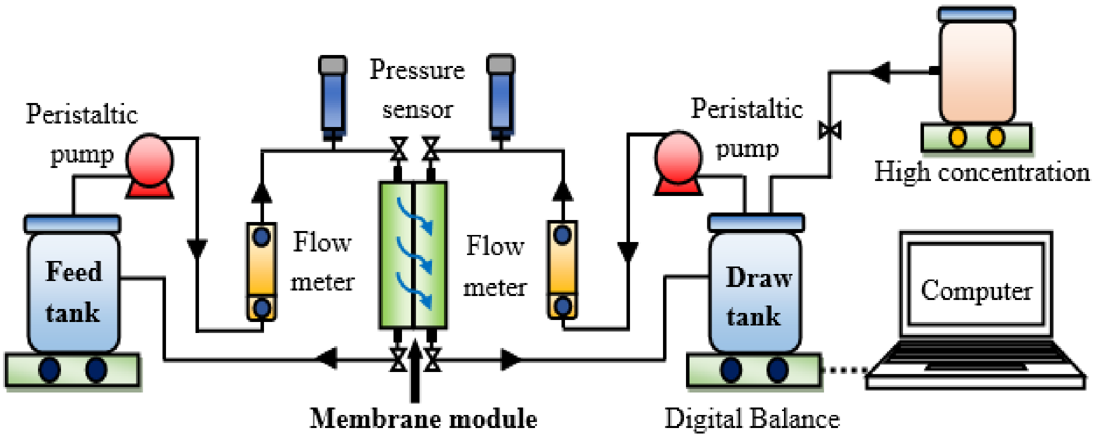

Figure 2.3. The diaphragm of FO unit

Figure 2.4. FO membrane module

2.2.4.2 Difference of NaCl concentration as draw solution

The water flux was analyzed with DI water and BSA solution concentration at 1 gL^{-1} in the feed side (FS) of membrane. NaCl concentration used as draw solution (DS) were 0.5, 1.0, 1.5 and 2 M of NaCl, respectively. The FS and DS flow was operated in co-current mode with 0.1 cm/s of velocity in both sides and test at room temperature (25±1 °C).

2.2.4.3 Difference of cross flow velocity

The water flux was analyzed using DI water and BAS solution concentration at $1gL^{-1}$ in the feed side (FS) of membrane. NaCl concentration used as draw solution was 2 M. The FS and DS flow were operated in co-current mode. The different cross flow velocity were 0.1, 0.3 and 0.7 cm/s.

2.2.4.4 Difference of temperature

The water flux was analyzed used DI water and BAS solution concentration at 1gL^{-1} in the feed side (FS) of membrane. The different temperature at 25±1, 35±1 and 45±1 °C was used to conduct the experiment with 2 M NaCl as draw solution. The FS and DS flow in co-current mode were operated at 0.7 cm/s.

2.2.5 Protein concentrate from tuna cooking juice by FO processes

Tuna cooking juice was obtained from Tropical Caning (Thailand) Public Company Limited, (Hat Yai, Thailand). The samples were prepared for each experiment (5 liters) and stored in plastic bottles at -20 °C until for experimental. The prepared sample were kept overnight at 4 °C until before filtration. The CTA modification membrane was tested for protein in tuna cooking juice concentrated. The experiment used NaCl 2 M as draw solution. The FS and DS flow operated in co-current mode at 0.7 cm/s under room temperature of 25±1°C. The protein concentration from tuna cooking juice were collected every 30 minute and determined following Lowry method (1951).

2.2.6 Fouling behavior

The analysis of fouling behavior was explored for each experiment. The graph of J_W, $\Delta\pi$ and operating time was presented. The evolution of these experiments were classified and determined. The confirmations of fouling were characterized by SEM.

Chapter 3

Result and discussion

3.1 Plasma treatment and grafting polymerization

3.1.1 Effect of plasma treatment

The contact angle and hydrophilicity of samples reduced after CO_2 plasma treatment as showed in Table 3.1. It could be concluded that the increase of hydrophilicity reached almost a constant value after 10 minutes of plasma exposure. The reduction of the contact angle presented from 64.04±3.13° to 18.51±1.74° and 9.38±0.00° for 10 minutes and 25 minutes at 20 watts, respectively. All further experiments were therefore conducted with membranes exposed for 10 minutes and 25 minutes of CO_2 plasma irradiation. The reductions correlated with high power and longtime exposure. The CO_2 plasma gas treatment was optimized during the power discharge and exposure time of 10 minutes at 20 watts.

Table 3.1. The contact-angle results of the untreated membrane, treated membrane and standard deviations for each experiment. (n=6)

Exposure time	**Contact angle (◦) (Average±SD) for each plasma power**			
	10 Watts	**20 Watts**	**30 Watts**	**50 Watts**
0	64.04±3.13	64.04±3.13	64.04±3.13	64.04±3.13
5	31.21±1.42	28.98±2.07	27.55±2.07	20.62±1.16
10	20.38±1.91	18.51±1.74	13.89±1.67	31.18±2.82
15	18.77±0.61	19.99±0.76	15.89±1.02	33.74±1.68
20	21.77±2.82	12.54±1.13	14.32±1.41	29.64±0.94
25	23.81±1.80	9.38±0.0	9.01±3.77	30.06±3.92

The optimizes discharge power and treatment time for modify membrane in this study were at 20 watts and 10 min, respectively. The result of contact angles of Ar plasma treatment showed in Table 3.2

Table 3.2. The contact angle of Ar plasma treated membrane at 20 watts (n=6)

Ar plasma treated (s)	**Contact angle (º)**
0	64.09±3.13
5	35.19±1.05
10	14.61±1.21
20	22.64±1.03
25	29.43±1.12

Table 3.2 presented the Ar plasma treatment on CTA membrane surface at 20 watts of power discharge. It was observed that the contact angle reduced from 64.09±3.13º to 14.61±1.12º at treatment time of 10 s (CTA;Ar), and it showed the optimized contact angle. The Ar plasma treatment on membrane surface could increase the hydrophilic of membrane surface. However, the contact angle of plasma treatment turned back contact angle overtime [83].

In addition, the type of gas-plasma treatment on CTA;CO_2 and CTA;Ar explained that the plasma gas CO_2 and Ar plasma treatment could increase the hydrophilicity on CTA membrane surface. For Ar (electropositive gases) and CO_2 (electronegative gases), the CO_2 had higher electronegativity, and the power discharge took place with the negative ion by electron. On the other hand, Ar plasma treatment had lower electronegativity. The higher of electron from Ar plasma could take place when it was activated on surface of membrane [97]. The Ar plasma showed a higher hydrophilicity of membrane surface. After CO_2 and Ar plasma treatments with discharge power of 20 watts and 10 minutes treatment time, is the optimizing to modify of membrane surface. The Ar plasma treatment showed higher hydrophilicity of the reduction of contact angle.

However, the higher power discharge and longer time of plasma treatment could destroy, etch and crack the surface of membrane confirmed from SEM image showed in the Figure 3.2 (b). The discharge power and shorter time for the optimizing of plasma treatment will be demonstrated in the next session (3.1.2).

3.1.2 Effect of plasma grafting polymerization

The hydrophilicity of membrane surface could be improved by plasma Ar gas treated on CTA membrane surface of discharge power at 20 watts. The contact angle measurements were used to identify the hydrophilicity of plasma grafting polymerization on CTA membrane surface. Table 3.3 showed the reduction of the contact angle presented from 64.04$\underline{+}$3.13° to 36.43$\underline{+}$1.40°, 27.43±0.24° for CTA; Untreated, CTA; Ar+AAc and CTA; Ar+TiO_2 membranes at 10 seconds. The Ar plasma treatment grafting polymerization of time at 10 seconds is the optimizing for modify of membrane surface. All results of contact angle plasma grafting polymerization showed the reduction of contact angle and the increase of hydrophilic of membranes surface. The plasma grafting polymerization increased the hydrophilic of membrane surface. This could change the properties of hydrophilic-chemical functional group like -COOH or -OH membrane [2, 10, 11].

Table 3.3. The condition of CTA membrane modification with Ar plasma AAc and TiO_2 grafting polymerization at 20 watts.

Time (s)	**Contact Angle (°)**	
	AAc	**TiO_2**
CTA;Untreated	64.04±3.13	64.04±3.13
5	44.89±3.27	43.21±2.37
10	36.43±1.40	27.43±0.24
15	42.99±2.65	35.86±1.00
20	47.31±1.62	42.08±1.91

The optimizing of Ar plasma grafting polymerization is at 10 seconds. The result of contact angle of CTA; Ar+AAc and CTA; Ar+TiO_2 membranes showed higher reduction of contact angle and high hydrophilic on membrane surface. This study on hydrophilic of membrane surface is used to analyze the characterization of membrane surface showed in the next session (3.2).

3.2 The characterization of membrane

3.2.1 Contact angle

Figure 3.1 (a, b and c) showed the contact angle which reduced from 64.04±3.13º to 18.51±1.74º and 14.61±1.21º for CTA;CO_2 and CTA;Ar membranes, respectively. The CTA;Ar membrane showed higher reduction of contact angle thane CTA;CO_2 membrane. Figure 3.1 (d, e) showed the image of contact angle reduced from 64.04±3.13º to 36.43±1.40º and 27.43±0.24º for CTA; Untreated, CTA; Ar+AAc and CTA; Ar+TiO_2 membranes, respectively. After using plasma modification on CTA membrane surface, there was the reduction of contact angle. The CTA of membrane surface modified with the Ar plasma TiO_2 grafting polymerization is considered the best for hydrophilicity.

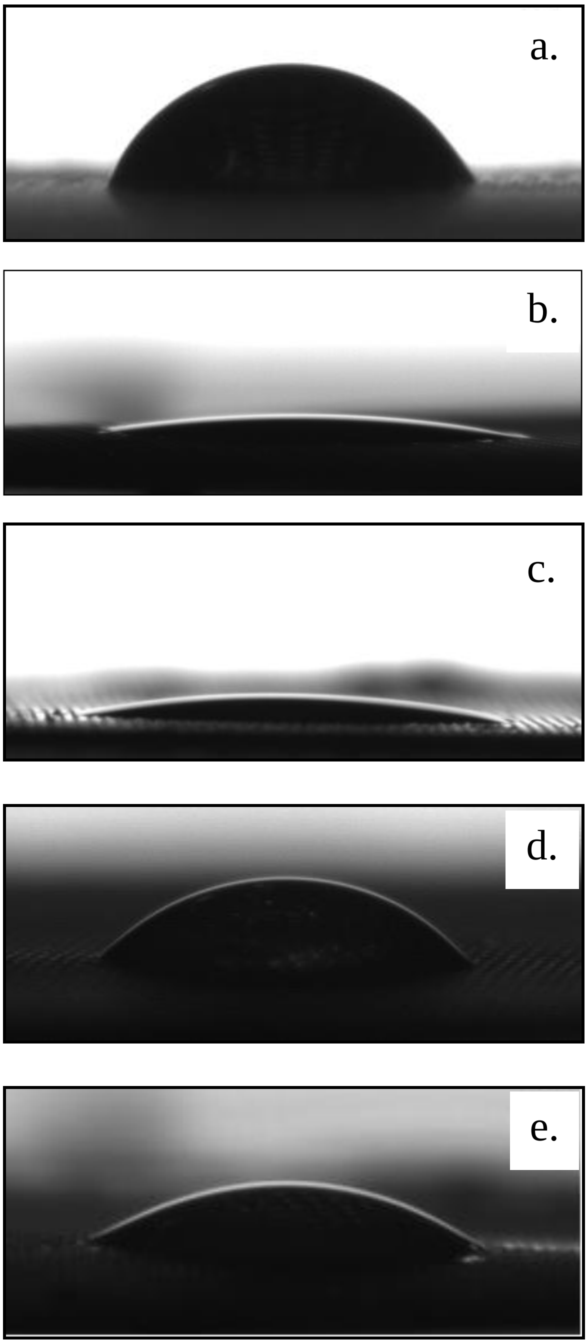

CTA;Untreated
CA left average = 64.00 °
CA right average = 63.99 °

CTA;CO$_2$
CA left average = 18.34 °
CA right average = 18.33 °

CTA;Ar
CA left average = 14.61 °
CA right average = 14.61 °

CTA; Ar+AAc
CA left average = 36.44 °
CA right average = 36.43 °

CTA; Ar+TiO$_2$
CA left average = 27.43 °
CA right average = 27.43 °

Figure 3.1. The images of contact angle of CTA membrane**;** (a) CTA;Untreated (b) CTA;CO$_2$ (c) CTA;Ar (d) CTA; Ar+CO$_2$ (e) CTA: Ar+TiO$_2$

3.2.2 SEM analysis

The SEM morphology characterization of CTA membrane was studied by using SEM analysis showed in Figure 3.2 (a). The figure displayed the asymmetric and properties of FO membrane which had selectively thin layer, approximately 10 µm and had a polyester mesh embedded material for mechanical support. The top layer was a smooth and densely selective layer. The overall thickness of the FO membrane was less than 50 µm [31]. Figure 3.2 (b), after modification of membrane surface, the CTA;CO_2 and CTA;Ar membranes showed the top layer which increased the roughness due to the etching membrane on its layer. The top layer of membrane surface seen large a void and cracked of membrane surface. The higher of power discharge and longer-time treatment could destroy the surface of membrane and could not change the surface properties of membrane [30]. However, the SEM image of CTA; Ar+AAc and CTA; Ar+TiO_2 membranes showed in Figure 3.2 (c) that it can be seen what was coated top layer of membrane was a smooth layer and was a new material grafting with AAc [83]. Figure 3.2 (d), the SEM image of membrane surface was a smooth layer membrane, and it was coated of TiO_2 nanoparticles formed on a top layer membrane [87]. This result was similar to another research in SEM of TiO_2 nanoparticle coated on surface of membrane. Figure 3.2 (e, f) clearly showed the image of TiO_2 formed on the top layer and a smoot layer on membrane surface which could increase the hydrophilic of membrane surface for higher flux and lees membrane fouling [87, 95].

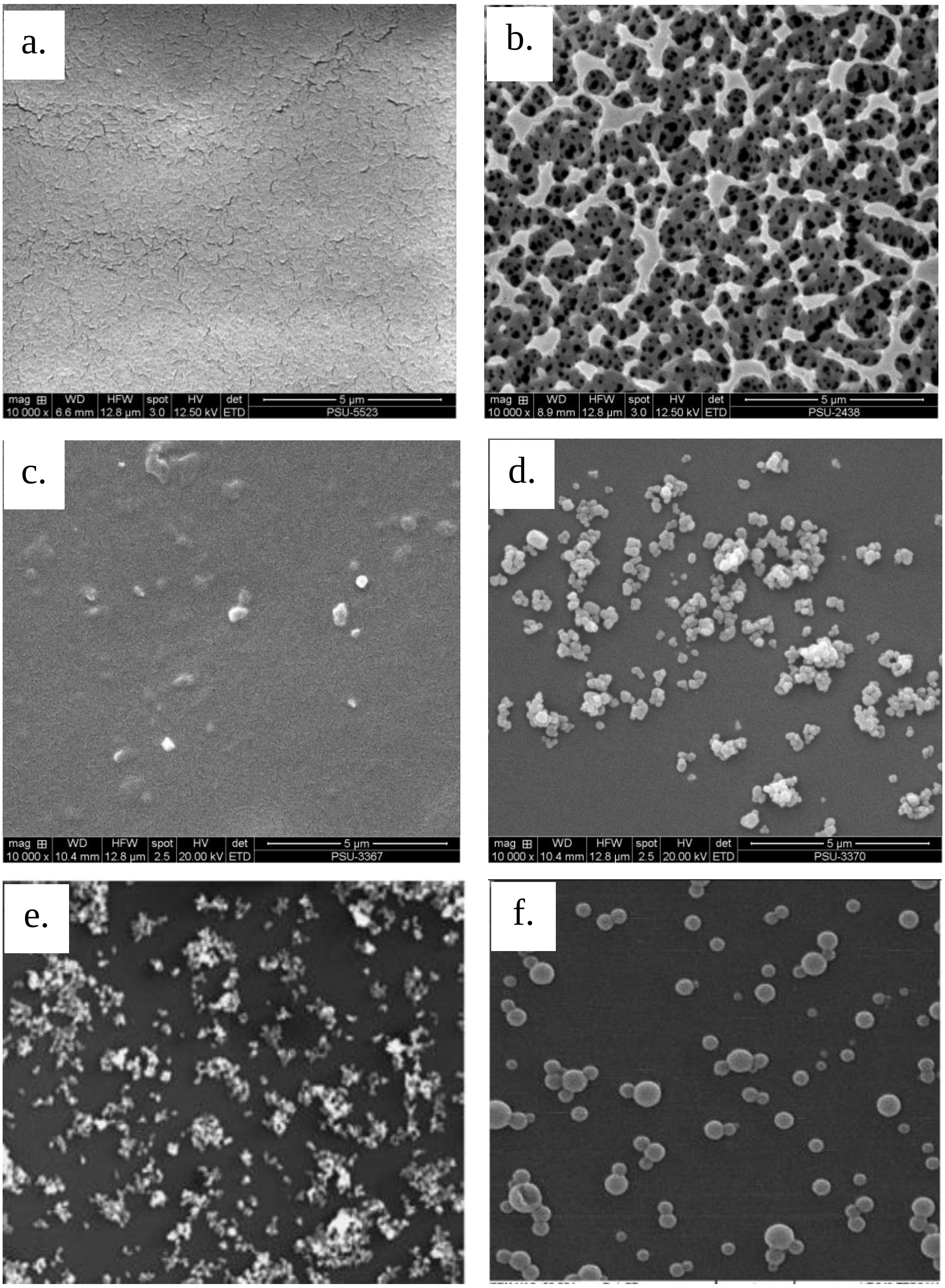

Figure 3.2. SEM image of plasma treatment and grafting polymerization onCTA membrane surface (a) CTA;Untreated (b) CTA;CO$_2$ (c) CTA;Ar+AAc (d) CTA; Ar+TiO$_2$ (e) TiO$_2$ coated on PES membrane [87] (f) TiO$_2$ on PES membrane [95]

3.2.3 FTIR measurement

The FTIR results of plasma treatment on CTA of membrane surface were presented in Figure 3.3. The CTA; Untreated membrane indicated the functional groups of –C-O stretching, Acetate -C-C-O- stretching, –C=O stretching, and –O-H stretching with absorption band wave number detected at 1042.1, 1232.6, 1742.1 and 3371 cm^{-1}, respectively. The CTA;CO_2 and CTA;Ar membranes treatment presented the same band of CTA;Untreated membrane and appearance of C=C or C≡C stretching,–C-H stretching and the wide peak of O-H stretching on the membrane surface. Subsequently, the element content of O and N increased with the increase of plasma-treatment time due to the surface oxidation [12].

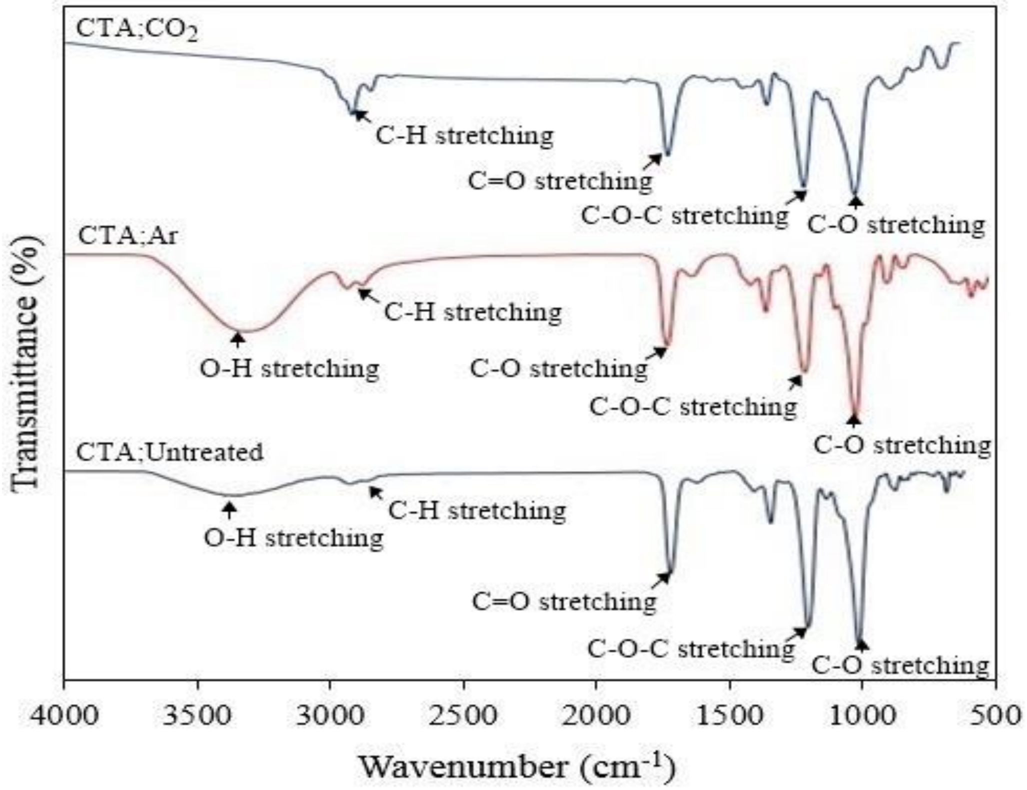

Figure 3.3. FTIR-ATR results plasma treatment on CTA membrane, CTA:Untreated, CTA:CO_2 and CTA;Ar.

From Figure 3.3, the possible assignments of the significant FTIR bands (cm^{-1}) appearing after CO_2 and Ar plasma modification changed the chemical properties of membrane surface of functional group, –COOH and –OH, to be their derivative with more hydrogen bonding. It can be concluded that the changing of surface structure of CTA and the surface oxidation caused the increase of polarity with -OH. The carbonyl groups were etched in the chain of CTA membrane at the densely top layer and changed to C=C, C=N. This result was further found in more capability of hydrogen bonding.

In addition, the Ar plasma modification of hydrophilicity on CTA membrane surface with AAc and TiO_2 grafting polymerization were analyzed its chemical functional group by FTIR-ATR. The FTIR-ATR frequency range of wave number 400- 4000 cm^{-1} was presented in Figure 3.4. The absorbance of CTA;Untreated membrane was similar to CTA;Ar+AAc and CTA;Ar+TiO_2 grafting polymerization membrane surface of wave number which was 1042.12 cm^{-1} (C-O stretching), 1230.83 cm^{-1} (C-O-C asymmetric stretching), 1742.70 cm^{-1} (C=O stretching) and 3406.04 cm^{-1} (O-H stretching). They all corresponded to the characteristic of functional group of acetate group in cellulose acetate (CA). The CTA;Ar+AAc membrane absorbed at 3472.21 cm^{-1} and 1733.71 cm^{-1} (C=O stretching) of the carboxylic group. This absorbance of O-H group entirely decreased after plasma treatment. The CTA;Ar+TiO_2 membrane which absorbed below 800 cm^{-1} bonded oxygen atom of the functional group of coordination Ti^{4+} cation of –COOH and -OH group to be their derivative with hydrogen bonding and the hydroxyl group [93,95]. There were also the TiO_2 grafted or coated on membrane surface as showed in Figure 3.5. The polymer of membrane surface was ion Ti^{4+} connected with two oxygen atoms of carboxyl group (-COOH) [12].

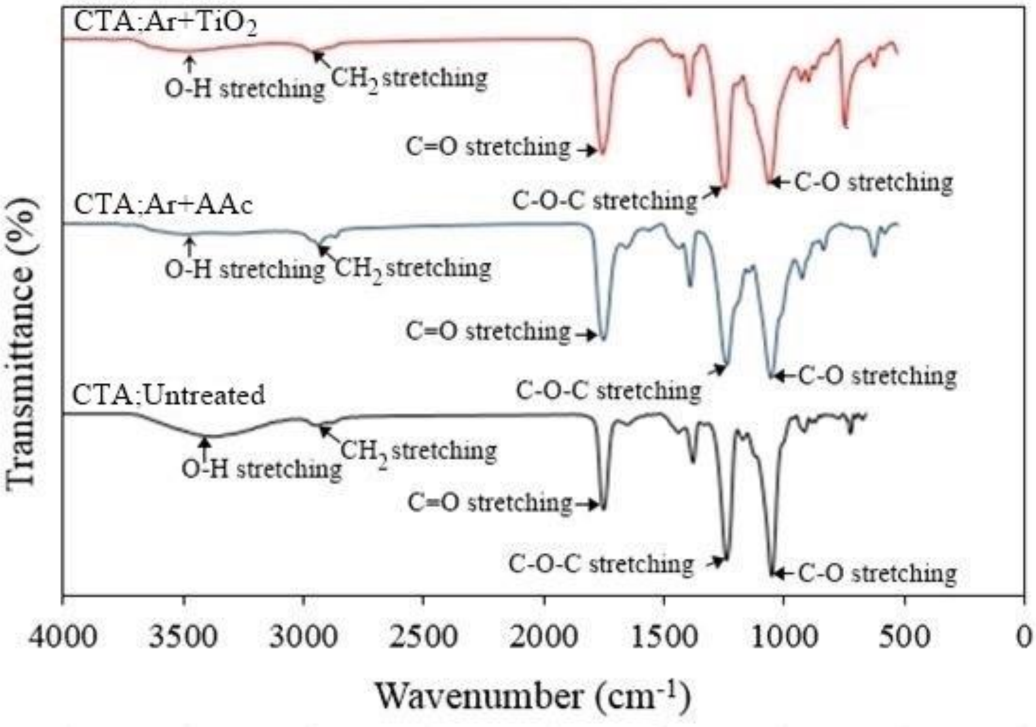

Figure 3.4. The FTIR-ATR of the Ar plasma grafting polymerization on membrane surface at power 20 watts of time in 10 seconds; CTA; Untreated, CTA; Ar+AAc and CTA;Ar+TiO_2

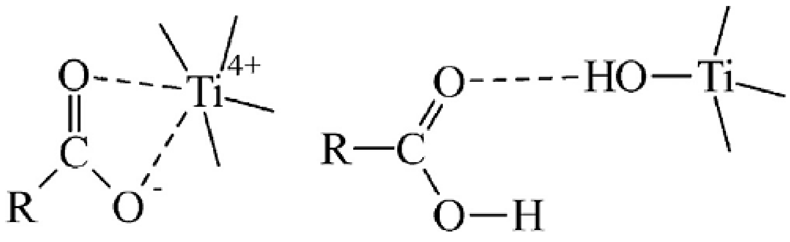

Figure 3.5. The transformation of TiO_2 coated on membrane surface [93].

3.2.4. AFM analysis

The AFM was used to study the characteristic of roughness of membrane surface. Figure 3.6 presented the roughness of the CTA;Untreated, CTA;Ar+AAc and CTA;Ar+TiO_2 membranes, respectively. Figure 3.6 (a), AFM image, was a smooth on the top layer of CTA;Untreated membrane. Figure 3.6 (b) and (c) showed the increasing of the roughness of plasma grafting polymerization membranes. Table 3.4 described the roughness analysis. The mean roughness (R_a) was 5.52 nm, 12.25 nm and 14.54 nm for CTA;Untreated, CTA;Ar+AAc and CTA;Ar+TiO_2, respectively. The root mean square (R_{ms}) was 3.02 nm, 8.35 nm and 9.14 nm for CTA;Untreated, CTA; Ar+AAc and CTA; Ar+TiO_2, respectively. The maximum vertical distance (R_{max}) was the roughness which the similar trends increased for plasma grafting polymerization. The results revealed that the roughness of plasma treated membrane increase compared with CTA;Untreated membrane. This result was agree with the report of Mongnifar et al., (2014) [95]. Therefore, the plasma modification of membrane surface should be applied to change the chemical functional group of hydrophilic of membrane surface in order to enhance flux and reduce the membrane fouling [19]. For hydrophilicity of membranes, the roughness should be increased to adsorb the foulant at the peak, less attached at the valley.

.

Table 3.4. The surface roughness of untreated and plasma grafting polymerization membranes

Membranes	**R_a (nm)**	**R_{ms} (nm)**	**R_{max} (nm)**
CTA;Untreated	5.52	3.02	103
CTA;Ar+AAc	12.25	8.35	162
CTA;Ar+TiO_2	14.54	9.14	190

The mean roughness (R_a)
The root mean square (R_{ms})
The maximum vertical distance (R_{max})

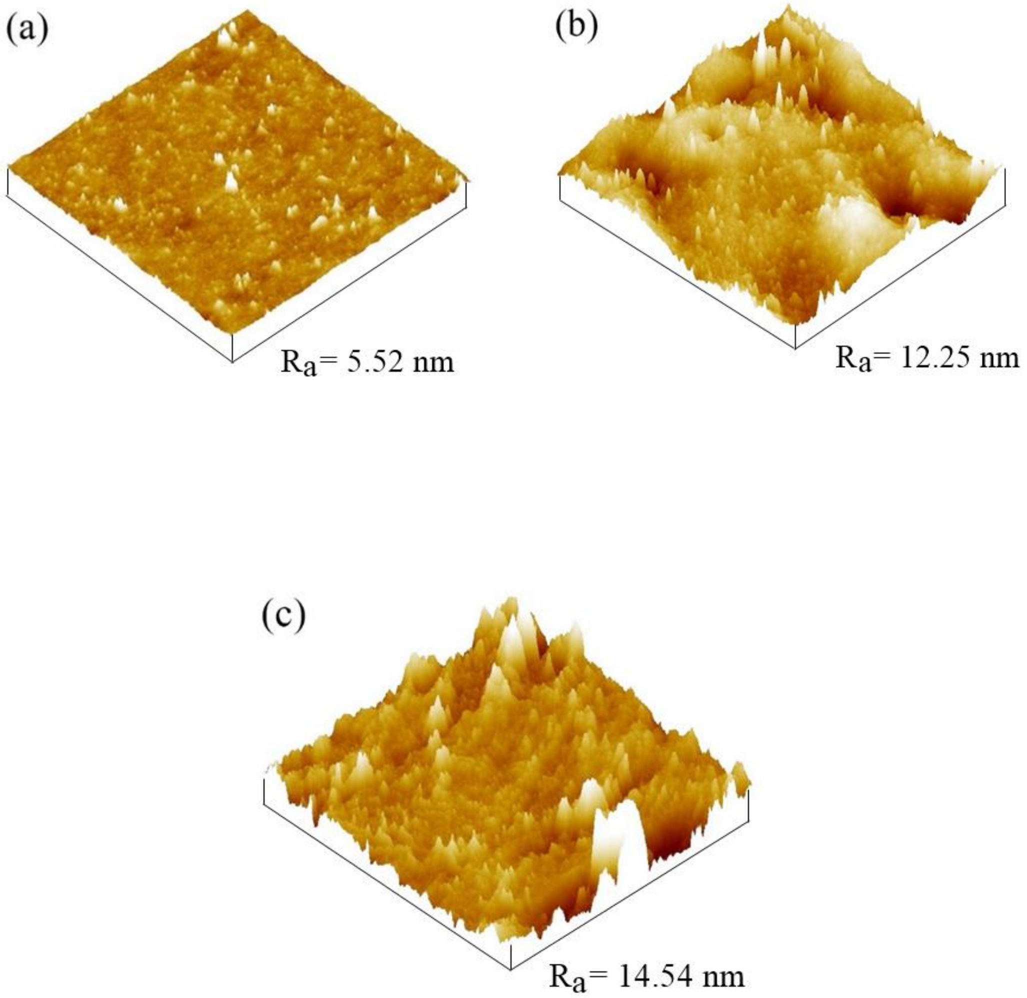

Figure 3.6. 3D image of CTA membrane grafting polymerization (a) CTA;Untreated (b) CTA;Ar+AAc (c) CTA;Ar+TiO$_2$.

3.2.5 XPS analysis

The XPS high resolution of C1s spectrum of the plasma AAc and TiO_2 grafting polymerization was presented in Table 3.5 that the spectrum of C1s of CTA;Untreated, CTA;Ar+AAc and CTA;Ar+TiO_2 plasma modification membrane showed in five peaks was corresponding to C-C, C-O, C-O-C, C=O and O-C=O functional group. After Ar plasma grafting polymerization, it was observed that the hydrophilic of functional group corresponded to hydroxyl C-O-C or –OH increasing from 20.4 % to 20.7 % and 28.4 % for CTA; Untreated, CTA; Ar+AAc and CTA;Ar+TiO_2, respectively. The functional group corresponded to the functional group of carboxyl of O-C=O or –COOH increasing from 2.9 % to 11.6 % and 13.0 % for CTA; Untreated, CTA;Ar+AAc and CTA;Ar+TiO_2, respectively. The narrow scan of C1s peak that confirmed of the hydrophilic functional group was a hydroxyl C-O-C or -OH and carboxyl O-C=O or –COOH.

Table 3.5. The XPS high resolution of C1s spectrum

Type	**C1s (%)**				
	C-C	**C-O**	**C-O-C**	**C=O**	**O-C=O**
CTA;Untreated	34.8	12	20.4	2.9	2.9
CTA;Ar+AAc	44.2	15.5	20.7	7.9	11.6
CTA;Ar+TiO_2	33.7	15.4	28.4	9.4	13.0

Figure 3.7. showed the high resolution spectrum of C1s peak of plasma grafting polymerization that confirmed the increase of hydrophilic functional group membrane at 284.8 eV (C-C), 285.6 eV (C-O), 286.7 eV (C-O-C), 287.9 eV (C=O) and 289.2 eV (O-C=O), respectively.

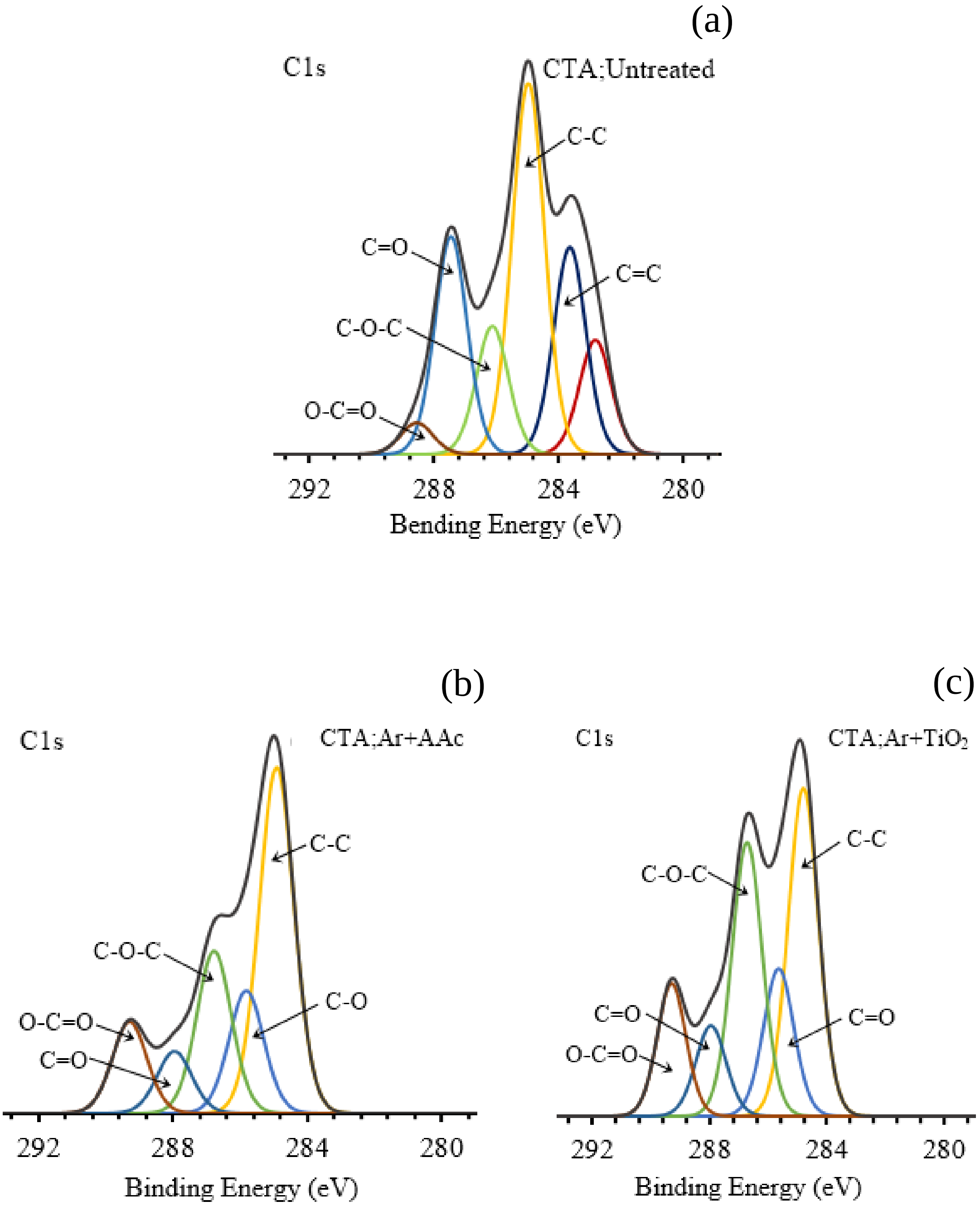

Figure 3.7. C1s spectrum high resolution (a) CTA;Untreated (b) CTA;Ar+AAc (c) CTA;Ar+TiO_2.

It was found that the plasma modification was able to increase the hydrophilicity of membrane surface. The modification of CTA membrane surface by plasma treatment and grafting polymerization method was strongly recommended by many researchers to improve the hydrophilicity of membrane surface. The chemical function of membrane surface changed the carboxyl group of –COOH and –OH group. The high resolution of C1s peak increased the hydrophilicity functional group with hydroxyl C-O-C or -OH and carboxyl O-C=O or –COOH group [91, 94].

3.3 The performance of system

3.3.1 The water permeable coefficient

The characteristic of a commercial FO membranes made from cellulose triacetate (CTA) from HTI had been widely used in FO studies, as showed in Table 3.6 that the water permeability coefficient used commercial cellulose triacetate (CTA) to test the setup of bench-scale on laboratory system in cell unit. The water permeability coefficient was $2.1 \times 10^{-12} ms^{-1} Pa^{-1}$ while the result of salt rejection ranged between 88 %. The surface hydrophilic membrane showed at 64°

Table 3.6. Specifications of the commercial FO (CTA) from HTI

Characteristic of cellulose triacetate membrane	
Permeate coefficient ($ms^{-1} Pa^{-1}$)	12×10^{-12}
Salt rejection (%)	88
Contact angle (˚)	64

3.3.2 Water permeability coefficient and salt rejection

The effects of plasma treatment modification on CTA membrane surface with graft AAc polymerization and coatedTiO_2 on membrane water permeability (A) and salt permeability (B) were used in RO mode. The result was showed in Table 3.7. It was found that, after the treatment on CTA membrane surface, the water permeability was 1.36 LMH and 1.78 LMH for CTA; Ar+AAc and CTA; Ar+TiO_2. The water permeability of plasma treated is higher than untreated membranes. While the plasma grafted polymerization is lower in salt permeability than both plasma treated and untreated CTA membrane. The salt rejections of feed NaCl 10 mM were 89 % and 91 % for CTA; Ar+AAc and CTA; Ar+TiO_2 membranes.

Table 3.7. Water permeability coefficient and salt rejection in RO

Membrane	Water permeability, A (LMH)	Salt permeability, B (LMH)	% Salt rejection
CTA;Untreated	0.74	0.68	88
CTA;CO_2	1.70	11.50	23
CTA;Ar	1.80	10.34	27
CTA;Ar+AAc	1.36	0.85	89
CTA;Ar+TiO_2	1.78	0.74	91

In addition, the water permeability of modified membrane both of plasma treatment and grafting polymerization showed the higher water permeability than the untreated membrane. The hydrophilicity of membrane surface that confirmed from CA, FTIR-ATR, AFM results was increased significantly. The plasma treatment and plasma graft polymerization of AAc and TiO_2 on the CTA membrane surface can increase the salt permeability. However, the salt rejection was decreased after plasma treatment. While the salt rejection of the plasma grafted membrane increased. The increase of the salt permeability of the plasma treated membranes correspond to the enlargement of void on the membrane surface that is confirmed from the SEM image in Section of 3.2.2.

3.3.3 The water flux and reverse salt flux in FO

Table 3.8 presented the comparison of the water flux and the reverse salt flux used feed DI water and feed 2 M NaCl as the draw solution in experiment in FO mode. For the performance of CTA;Ar+AAc and CTA;Ar+TiO_2 membranes, it was observed that the water flux increased higher comparing with the CTA;Untreated membrane. The water flux of feed DI water was 5.08 LMH, 8.12 LMH and 9.22 LMH for CTA;Untreated, CTA;Ar+AAc and CTA;Ar+TiO_2, respectively. The modification of membrane an increase hydrophilic of membrane surface with increase of the water flux. The water flux of plasma AAc and TiO_2 grafted polymerization membrane surfaces was enhanced according to the increase of the hydrophilicity of membrane surface [12].

Table 3.8. The FO performance of different plasma treatment and grafting on membrane

Plasma treatment	Water flux (J_w: LMH)	Salt reverse flux (J_S;mol. gMH)
CTA;Untreated	5.08	0.027
CTA;CO_2	3.80	1.560
CTA;Ar	3.92	1.510
CTA;Ar+AAc	8.12	0.025
CTA;Ar+TiO_2	9.22	0.020

The plasma treatment showed the increase of hydrophilicity and higher water permeability. However, it also showed a lower water flux and higher salt reverse flux comparing with CTA;Untreated membrane based on the SEM image that showed large a void of membrane surface, lower salt rejection and higher reverse salt flux.

3.3.4 Effect of operating condition on water flux and salt reverse flux

3.3.4.1 Effect of different NaCl concentration as draw solution

The operating conditions of FO process, the systematic experiment had studied the effect of feed NaCl concentration between 0.5 M – 2 M as draw solution on water flux and salt reverse flux. The flux obtained from different draw solution was showed in Figure 3.8 (a). The water flux increased both feed solution DI water and BSA solution by increasing the concentration as draw solution from NaCl 0.5 M to 2 M. The water flux of DI water increased from 4.34 LMH to 6.63 LMH, and the BSA flux increased from 3.93 LMH to 6.11 LMH for feed NaCl 0.5 M and 2 M as draw solution. The high water fluxes were from a high concentration as a greater osmotic pressure. However, considering from Figure 3.8 (b) that the high osmotic pressure with high concentration can also increase the salt leakage from draw solution across semi-permeable membrane. The reverse salt from feed DI water increased from 1.45 gMH to 3.57 gMH for 0.5 M to 2 M NaCl draw solution, and the reverse salt from feed BSA solution increased from 1.34 gMH to 3.53 gMH for NaCl 0.5 M and 2 M, respectively. The reverse salt flux was one of the phenomenon that could decrease the water flux. The decrease of water flux could explain the cause of internal concentration polarization (ICP) from feed draw solution [12].

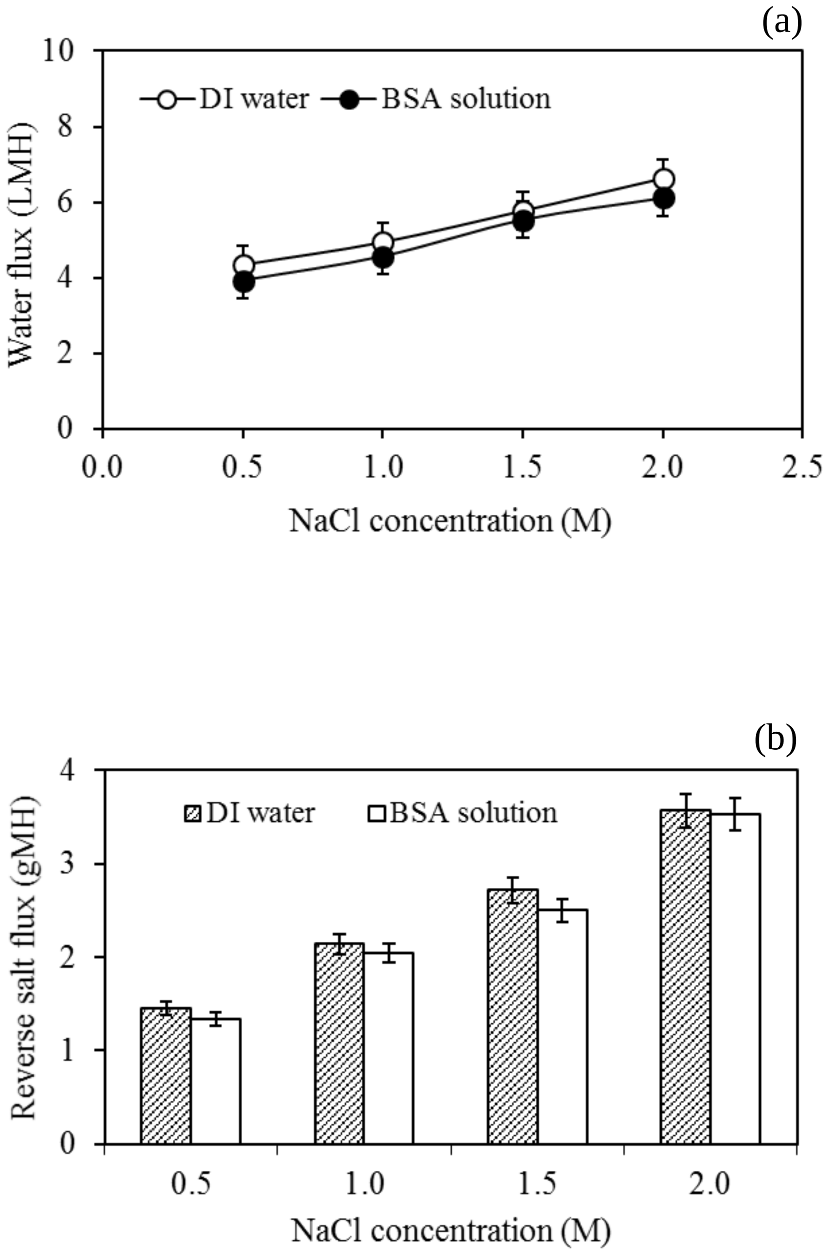

Figure 3.8. The performance of different NaCl 0.5- 2 M as the feed draw solution; using DI water and BSA solution as feed solution, co-current mode as cross-flow velocity at 0.1 cm/s, room temperature at 25±1 ºC (a), water flux (b), salt reverse flux.

From Figure 3.8, the optimizing of draw-solution concentration was 2 M NaCl because the high flux and salt reverse flux were obtained. This condition was selected to operate in next session.

3.3.4.2 Effect of difference cross flow velocity

The effect of cross-flow velocity, in Figure 3.9 (a), showed that the water flux used a feed constant at NaCl 2 M as draw solution, after filtration by changing the cross-flow velocity from 0.1-0.7 cm/s, both DI water and BSA solution. It was observed that the water flux increased from 5.47 LMH to 7.26 LMH as DI water and 4.57 LMH to 6.28 LMH as BSA solution for 0.1 cm/s and 0.7 cm/s respectively. The higher cross-flow velocity demonstrated the higher water flux. However, the salt leakage from draw solution presented in Figure 3.9 (b) was observed that the reverse salt flux increased with the increase of cross-flow velocity both of from feed DI water and BSA solution. These results showed higher reverse salt flux with the increase of cross-flow velocity since the constant form of draw solution could get higher osmotic pressure. The hydrodynamic shear force was to increase with the increase feed inside of flow rate. These processes were the reduction in ICP and ECP.

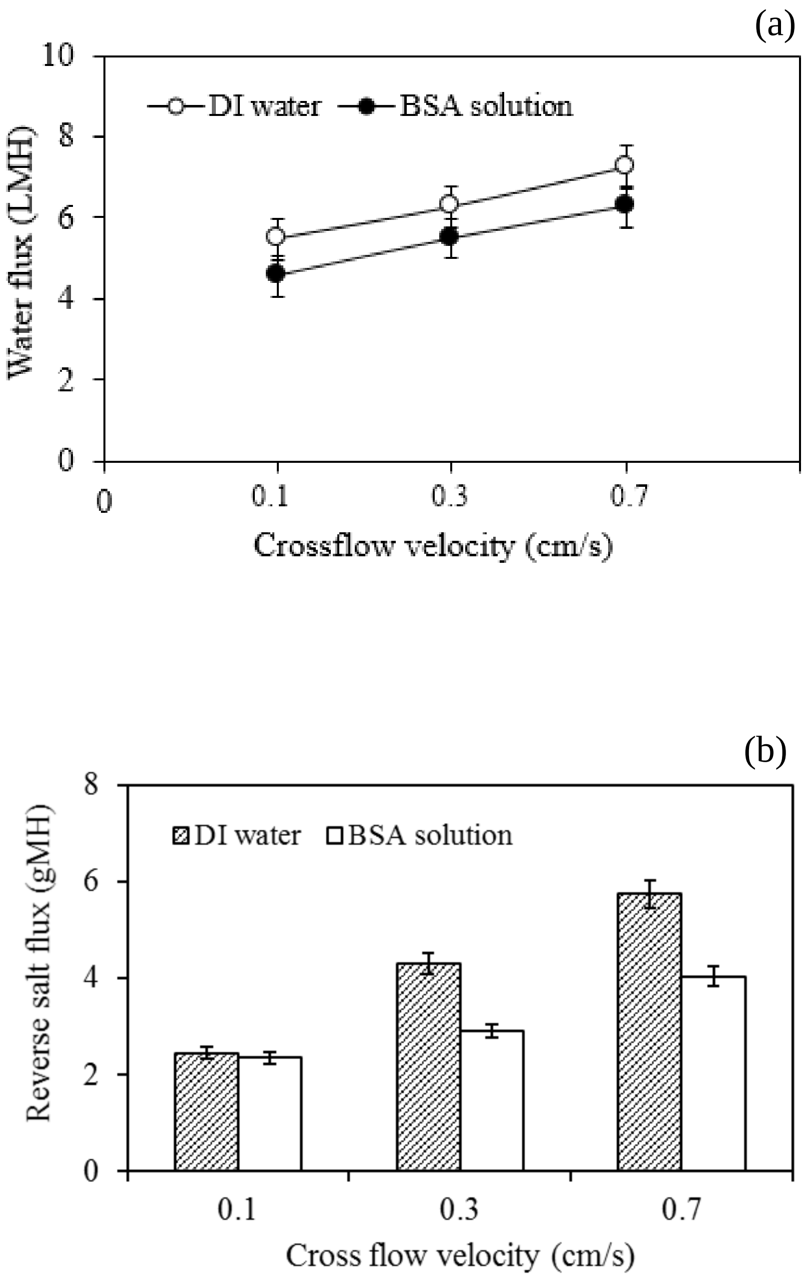

Figure 3.9. The performance of different co-current cross-flow velocity increasing 0.1, 0.3 and 0.7 cm/s (a) water flux (b) reverse salt used DI water and BSA solution as feed solution, NaCl 2 M as draw solution, room temperature 25±1 ºC.

3.3.4.3 Effect of different temperature

After the experiment in the different NaCl concentration as draw solution, the feed solution of NaCl 2 M as draw solution and a cross flow velocity were at 0.7 cm/s in this study. The effect of different temperature presented in Figure 3.10 (a, b) affected by feed different temperature on water flux was observed that the water flux and reverse salt flux increased with the increase of temperature from 25 ºC to 45 ºC, both feed solution, in the FO process. The water flux was increased from 6.78 LMH to 8.42 LMH for feed DI water and 6.28 LMH to 7.63 LMH for feed BSA solution as temperature 25 ºC to 45 ºC. The increase of temperature can decrease the viscosity of water leading to increase of water diffusivity through the membranes. The parameter's operation on temperature was a significant performance in FO processes. You et al,. (2008) [98] studied the feed solution between 20-40 ºC in FO process and observed that water flux increased in all temperatures. However, the reverse salt flux increased only with the increase of temperature.

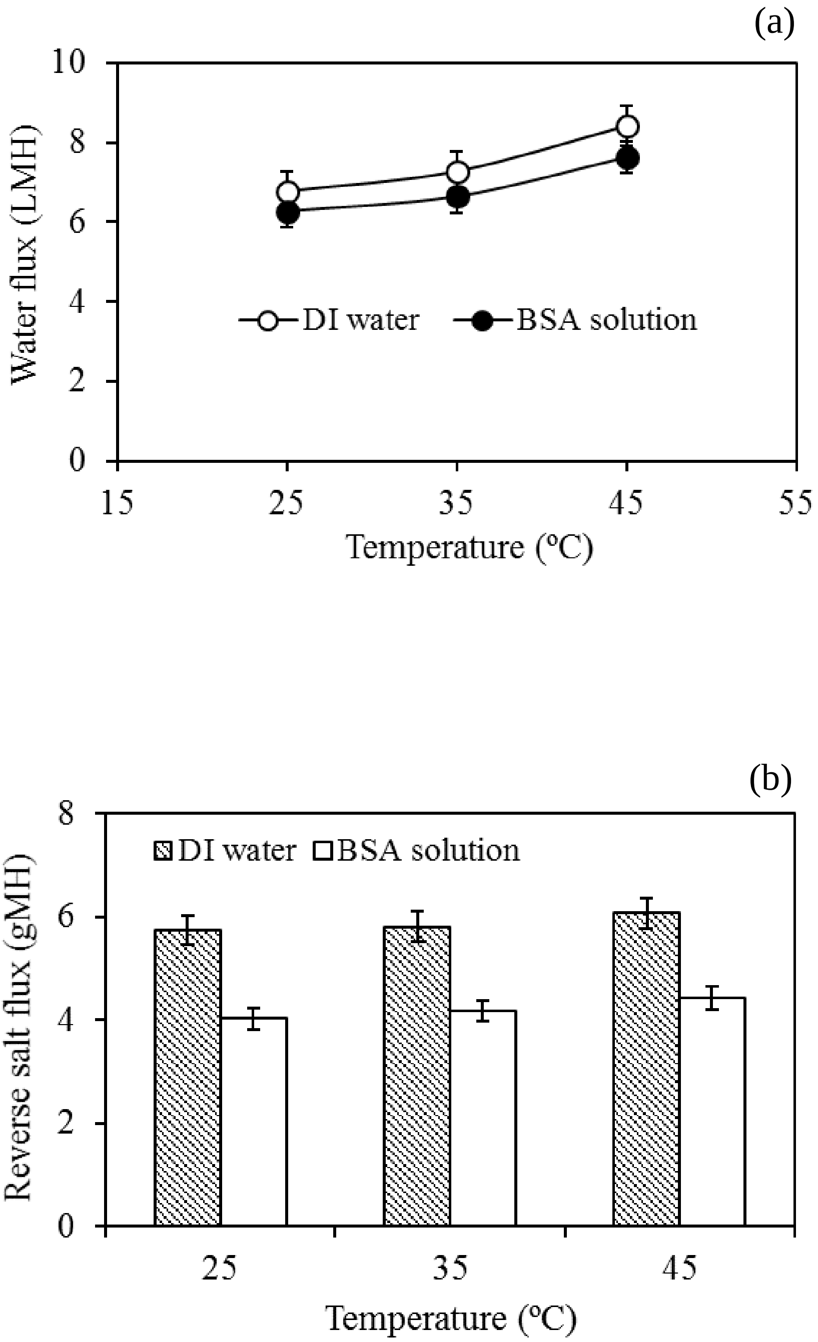

Figure 3.10. The performance of difference temperature between 20 to 45 °C; used DI water and BSA solution as feed solution; Co-current cross flow velocity 0.7 cm/s; NaCl 2 M as draw solution; (a) water flux (b) reverse salt flux.

3.3.5 The water flux of plasma treatment in long term in FO

From Figure 3.11, the results showed the decrease of water flux after the treatment by CO_2 plasma and the higher salt leakage. BSA solution filtration of the plasma treatment on membrane showed the lower water flux for 30% in the beginning, and there were more reverse salt flux than untreated membrane. However, after filtration for 420 minutes, the water flux of CTA:Untreated membrane decreased and got close to the water flux of treated membrane at 800 minutes. The plasma modification of CTA;CO_2 and CTA;Ar membranes surface for 10 minutes that should be improved was a protein antifouling. The hydrophilic of membrane surface could reduce interactions and decrease protein absorption [12]. In consequence, the separating performance for BSA solution could also be enhanced by CO_2 and Ar plasma treatment. It was, therefore, the treated CTA membrane at 10 minutes which was suitable for protein filtration.

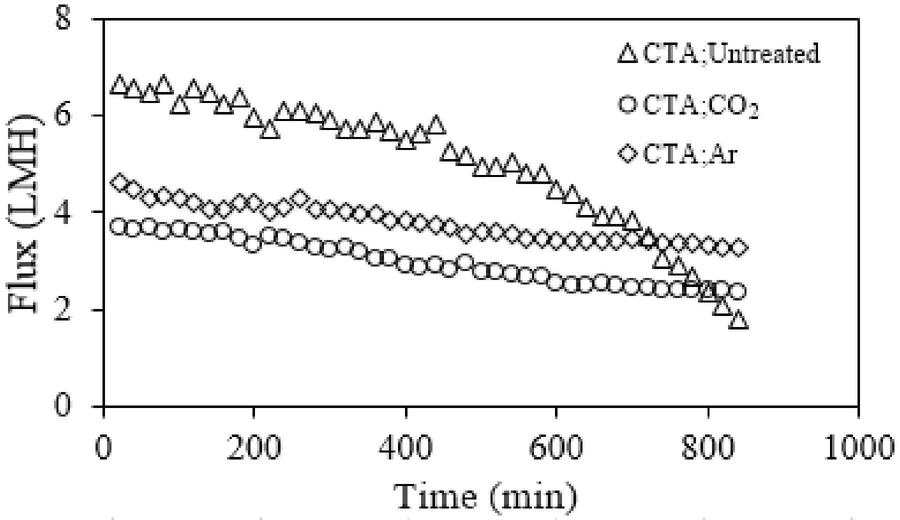

Figure 3.11. The duration fluxes and time; △CTA;Untreated, ○CTA;CO_2,◇CTA;Ar. The feed BSA solution of $1 gL^{-1}$ feed solution with difference membrane; used NaCl 2 M as the draw solution; Co-current cross flow at 0.7 cm/s; room temperature 25±1 ºC.

3.3.6 The water flux of plasma grafting polymerization in long term in FO

Figure 3.12 (a) presented the water flux after using different membrane filtration of BSA solution. The long-term water flux was observed that the flux slightly decreased and stayed constant at 500 minutes of CTA;Untreated membrane. In addition, the CTA; Ar+AAc and CTA; Ar+TiO_2 membranes were both showed higher flux of plasma modification comparing with CTA;Untreated membrane. These results were showed slightly the decrease of water flux. The plasma surface modification of membrane was increased the hydrophilicity of membrane. The increase of the hydrophilicity can reduce membrane fouling. All modification of membrane surface was higher hydrophilicity with the high water flux than CTA;Untreated membrane. The phenomena of membrane fouling from feed with the decline of flux obtained due to accumulation on selective layers.

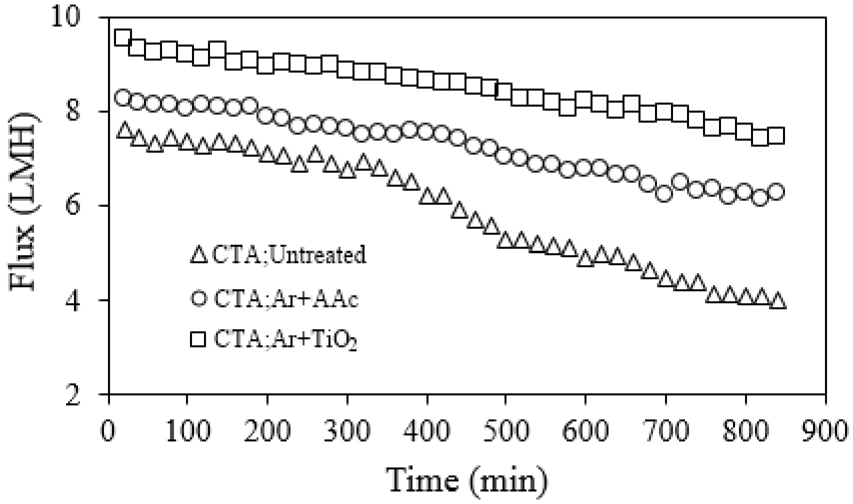

Figure 3.12. Effect of different Ar plasma grafting polymerization on water flux, △ CTA;Untreated,○ CTA;Ar+AAc and◇ CTA;Ar+TiO_2; The feed BSA solution of 1 gL^{-1} feed solution with different membrane; used NaCl 2 M as the draw solution; co-current cross flow at 0.7 cm/s; room temperature 25±1 °C.

3.4 Concentration of protein from tuna cooking juice

Figure 3.13 (a) presented the water flux of tuna cooking juice. After filtration of tuna cooking juice, it was clear that the water-flux averages were 2.36 LMH, 3.53 LMH and 4.16 LMH for CTA; Untreated, CTA; Ar+AAc and CTA; Ar+TiO_2, respectively. The water flux decreased for CTA; Untreated membrane. However, the water flux slightly decreased and stayed constant at 240 minutes made the modification of membrane surface higher comparing with untreated membrane.

The increase of hydrophilicity of membrane surface can reduce the membrane fouling and cause the protein absorption interacting between protein and membrane surface. However, membrane fouling caused from tuna cooking juice was probably composed of water soluble materials from gelatin, skin tuna fish and tuna fish on surface of membrane (ECP). In addition, Figure 3.13 (b) showed the protein recovery from tuna cooking juice, and it was found that the protein concentration form 5.5 % (w/v) to 9.71 % (w/v) and 10.30 % (w/v) for CTA; Ar+AAc and CTA; Ar+TiO_2 membranes at 300 minutes. Figure 3.13 (c) also showed the protein recovery of 76.43 % and 87.32 % for CTA;Ar+AAc and CTA;Ar+TiO_2, respectively.

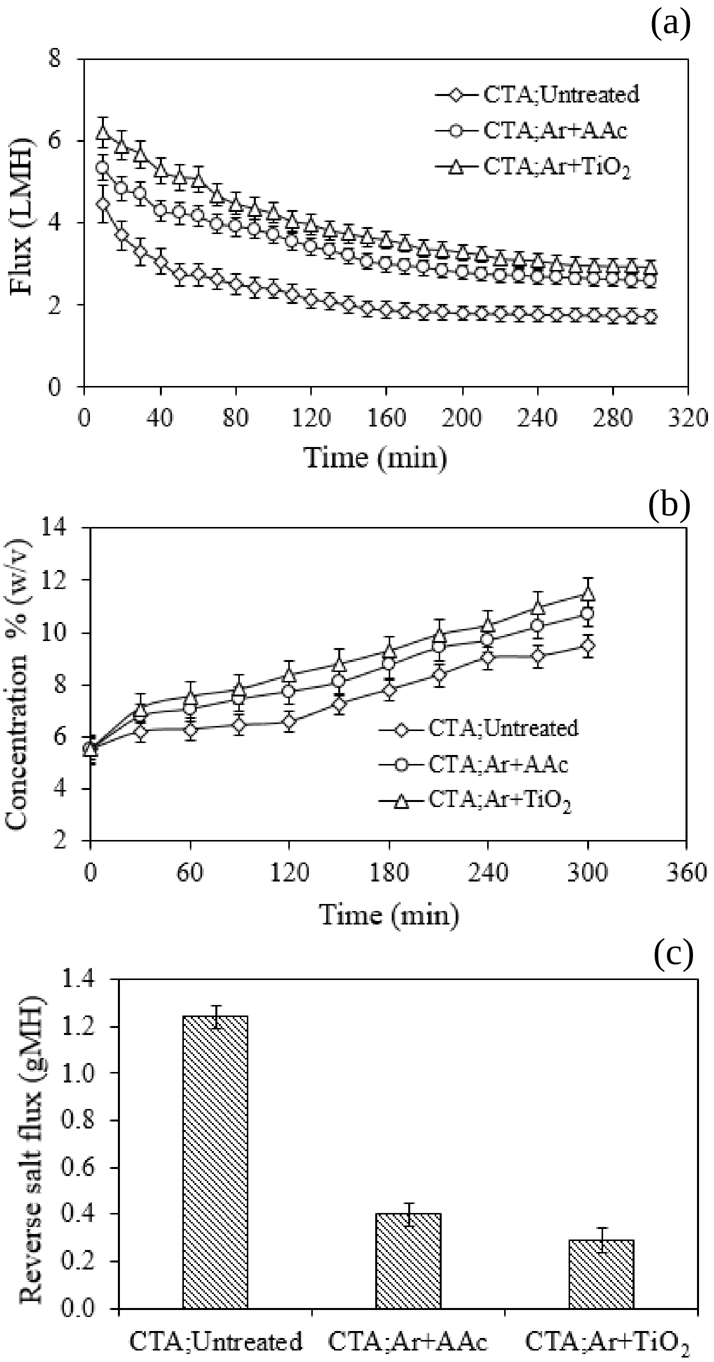

Figure 3.13. The filtration of tuna cooking juice with CTA;Untreated, CTA;Ar+AAc and CTA;Ar+TiO_2 ;(a) water flux (b) protein concentration (c) reverse salt flux; the feed solution of tuna cooking juice; co-current mode at cross flow velocity at 0.7 cm/s with NaCl 2 M as draw solution at room temperature 25±1 ºC.

3.5 Characteristic of tuna cooking juice

The physico-chemical characteristics of tuna cooking juice of feed and permeate after filtration in FO processes were presented in Table 3.11. The tuna cooking juice of TOC was 30.28 mg/L, COD decreasing from 23,280 to 1,955 mg/L, BOD decreasing from 7960 to 2.6 mg/L and TOC decreased 50 %, respectively.

Table 3.9. Physico-chemical characteristics of tuna cooking juice in FO process

Composition	**Tuna cooking juice**		
	Feed	**Permeate Draw**	**Concentrate**
pH	5.79	5.76	5.57
COD (mg/L)	23,280	1,955	30,220
BOD (mg/L)	7,960	2.6	10,130
Conductivity (mS/cm)	16.2	132.2	19
TOC (mg/L)	60.28	30.28	NA
Viscosity (mPa.s)	0.036	0.012	0.057

Chapter 4

Conclusion and future work

4.1 Conclusion

The plasma modification of CTA membrane surface for enhancing flux, salt leakage and concentration on protein recovery. The plasma treatment got improved to increase hydrophilicity of membrane surface. The contact angle reduced from 64.04±3.13° to 18.51±1.74° and 14.61±1.21° for CTA;CO_2 and Ar plasma treatment of power discharge at 10 minutes at 20 watts. The Ar plasma treatment showed higher reduction of contact angle comparing with CO_2 plasma treatment. The reduction of the contact angle was presented from 64.04±3.13° to 36.43±1.40°, 27.43±0.24° for CTA;Untreated, CTA;Ar+AAc and CTA;Ar+TiO_2 of power discharge of 10 seconds at 20 watts. The plasma treatment increases the hydrophilic of membrane surface which caused the change of the properties of hydrophilic chemical functional group like -COOH or -OH membrane. The result of roughness analysis was that the mean roughness (R_a) increased from 5.52 to 12.25 and 14.54 nm for CTA;Untreated, CTA;Ar+AAc and CTA;Ar+TiO_2. The high resolution of C1s peak justified the increase of hydrophilicity functional group with hydroxyl C-O-C or -OH and carboxyl O-C=O or –COOH group. The performance of Ar plasma TiO_2 grafting polymerization showed that the water permeability were 1.78 LMH and salt rejection were 91 %. The water flux in FO processes showed 9.74 LMH, and the reverse salt flux were 0.020 gMH.

The water flux of tuna cooking juice averages were 4.16 LMH, and salt reverse flux was 0.29 gMH. The protein concentration showed 10.30 % w/v, the percentage of recovery was 87.32 %. The COD decreased from 23,280 to 1,955 mg/L, and BOD decreased from 7960 to 2.6 mg/L and TOC decreased 50% respectively. However, the process standard significantly needs to be developed to the quality permit.

4.2 Future work

1. The low plasma discharge and shorter-time should be modified on membrane surface.
2. The modification of membrane surface should be developed on the synthesis of new membrane or modification to increase higher flux and low salt leakage.

Reference

1. Ministry of Commerce Thailand. 2014. (Online) Available http://www2.ops3.moc.go.th (25 January 2015)

2. Prasertsan, P.Wuttjumnong, P.Sophanodora and Choorit. 1998. Seafood Processing Industries within Songkla-Hat Yai Region: The Survey of Basic Data Emphasis on Wastes. *Songklanakarin Journal of Science and Technology*. 10: 447-451.

3. L. Vandanjon, S. Cros, P. Jaouen, F. Quéméneur and P. Bourseau. 2002. Recovery by nanofiltration and reverse osmosis of marine flavours from seafood cooking waters. *Desalination*. 144: 379–385.

4. K. Walhaa, R. B. Amara, P. Bourseau, P. Jaouen, 2009. Nanofiltration of concentrated and salted tuna cooking juices. *Process Safety and Environmental Protection*. 8, 7: 331–335.

5. Kasiwut, J. 2012. Antioxidative, Angiotensin I-Converting Enzyme (ACE) Inhibitory and Ca-Binding Activities of Peptides Produced from tuna Cooking Juice and Spleen Extract-Protease. Master Thesis. Prince of Songkla University.

6. K. Walha, R.B. Amar, A.Masse, P. Bourseau, M. Cardinal, 2011. Aromas potentiality of tuna cooking juice concentration by nanofiltration. *LWT- Food Science and Thehnology*. 44: 153-157.

7. K.C. Hsu, G.H.Lu and C.L.Jao 2009. Antioxidative properties of peptides prepared from tuna cooking juice hydrolysates with orientase (Bacillus subtilis). *Food Research International*.42: 647–652.

8. M. Hajiham and W. Youravonga. 2013. Concentration and Desalination of Protein Derived from Tuna Cooking Juice by Nanofiltration. *Jurnal Teknologi*. 65: 1-6.

9. M. D. Afonso, R. Borquez, 2002. Review of the treatment of seafood processing wastewaters and recovery of proteins therein by membrane separation processes- prospects of the ultrafiltration of wastewaters from the fishmeal industry. *Desalination* 142: 29-45.

10. Khetprathum. 2008. Production and Physicochemical Propertices of Fish Wash water in Surimi industry using Ultrafiltration and Spray dry. Master Thesis. Prince of Songkla University.

11. W. Bootluck, W. Khongnakorn and W. Youravong. 2014. Effect of Different Concentration of Draw Solution on BSA Recovery by Forward Osmosis. 3rd International Conference on Environmental Engineering, Science and Management. Bangkok, Thailand, 26–28 March, 2014.

12. W. Khongnakorn, W. Bootluck, W. Youravongc 2014. Surface Modification of CTA-FO Membrane by CO_2 Plasma Treatment. *Jurnal Teknologi*. 70:2, 71–75.

13. Mi, M. Elimelech. 2010. Organic fouling of forward osmosis membranes: Fouling reversibility and cleaning without chemical reagents. *Journal of Membrane Science*. 348: 337–345.

14. E. M. G.Castello, J. R. M. Cutcheon and M. Elimelech. 2009. Performance evaluation of sucrose concentration using forward osmosis. *Journal of Membrane Science*. 338: 61–66.

15. R. L. M. Ginnis and M. Elimelech. 2007. Energy requirements of ammonia–carbon dioxide forward osmosis desalination. *Desalination*. 207: 370–382.

16. Achilli, T. Y. Cath, E. A. Marchand and A. E. Childress. 2009. The forward osmosis membrane bioreactor: A low fouling alternative to MBR processes. *Desalination*. 239:10–21.

17. Achilli, T. Y. Cath and A. E. Childress a 2009. Power generation with pressure retarded osmosis: An experimental and theoretical investigation. *Journal of Membrane Science*. 343: 42–52.

18. G. Han, S. Zhang, X. Li, N. Widjojo and T.S Chung. 2012. Thin film composite forward osmosis membranes based on polydopamine modified polysulfone substrates with enhancements in both water flux and salt rejection. *Chemical Engineering Science*. 80: 219–231.

19. Emadzadeh, W. J. Lau, T. Matsuura, A. F. Ismail and M. R. Sisakht. 2014. Synthesis and Characterization of Thin film Nanocomposite Forward Osmosis Membrane with Hydrophilic Nanocomposite Support to Reduce Internal Concentration Polarization. *Journal of Membrane Science*. 449: 74–85.

20. Sujarit. 1997. Cultivation of yeast in Tuna cooking juice after Protein and Fat Separation. M.Sc. Biotechnology. University of Songklanakarin.

21. Sarabok and H.A. Kittikun. 1999. Enzymatic Hydrolysis of Tuna cooking juice for flavor sauce product. *Songklanakarin Journal Science and Technology*. 21:491-500.

22. M. Jatupornpipat. 1994. Optimization for Growth and Pigment /synthesis of Rhodocyclus gelatinosus R7 Cultivating in Tuna cooking juice. M.Sc. Biotechnology. University os Songklanakarin.

23. K. Kitrunkrote, S. Maneerut and T, Bourtoom. 2000. Development of Hight Protein tuna Soup Production from Tuna cooking juice. In Proceeding of Development and Engineering. *Proceeding*. 1-53.

24. K.Y. Wang, M.M. Teoh, A. Nugroho and T.S. Chung. 2011. Integrated forward osmosis–membrane distillation (FO–MD) hybrid system for the concentration of protein solutions. *Chemical Engineering Science*. 66: 2421–2430.

25. L. Shaffer, J. R.Werber, H. Jaramillo, S. Lin and M. Elimelech. 2015. Forward osmosis: Where are we now?. *Desalination*. 356: 271–284.

26. L. Chekli, S Phuntsho , H. K. Shon , S. Vigneswaran , J. Kandasamy and A. Chanan. 2014. A review of draw solutes in forward osmosis process and their use in modern applications. *Desalination and Water Treatment*. 43: 167-184.

27. D. Mehta, L. Gupta, and R. Dhingra. 2014. Forward Osmosis in India: Status and Comparison with Other Desalination Technologies. *International Scholarly Research Notices*. 9

28. Altaee, G. Zaragoza and H. R. V. Tonningen. 2014. Comparison between Forward Osmosis-Reverse Osmosis and Reverse Osmosis processes for seawater desalination. *Desalination*. 336: 50-57.

29. T.Y. Cath., A.E. Childress and M. Elimelech. 2006. Review: Forward osmosis: Principles, applications, and recent developments. *Journal of Membrane Science*. 281: 70–87.

30. K. Lutchmiah, A.R.D. Verliefde , K. Roest, L.C. Rietveld and E.R. Cornelissen. 2014. Forward osmosis for application in wastewater treatment: A review. *Water research*. 5 8: 1 7 9- 9 7

31. K.Y.Wang, T.S. Chung, J.J. Qin. 2007. Polybenzimidazole (PBI) nanofiltration hollow fiber membranes applied in forward osmosis process. *Journal of Membrane Science*. 300: 6–12.

32. K. Gerstandt, K.-V. Peinemann, S.E. Skilhagen, T. Thorsen and T. Holt. 2008. Membrane processes in energy supply for an osmotic power plant. *Desalination*. 224: 64–70.

33. S. Chou, L. Shi, R. Wang, C.Y. Tang, C. Qiu and A.G. Fane. 2009. Characteristics and potential applications of a novel forward osmosis hollow fiber membrane. Desalination. 261: 365-372.

34. Q. Yang, K.Y. Wang and T.S. Chung. 2010. Dual-layer hollow fibers with enhanced flux as novel forward osmosis membranes for water production. *Environmental Science and Technology*. 43: 2800-2805.

35. J. Su, Q. Yang, J.F. Teo and T.S. Chung. 2010. Cellulose acetate nanofiltration hollow fiber membranes for forward osmosis processes. *Journal of Membrane Science*. 355: 36–44.

36. Tiraferri, N.Y. Yip, W.A. Phillip, J.D. Schiffman and M. Elimelech. 2010. Relating performance of thin-film composite forward osmosis membranes to support layer formation and structure. *Journal of Membrane Science.* 367: 340–352.

37. Y. Yu, S. Seo, I.-C. Kim and S. Lee. 2011. Nanoporous polyethersulfone (PES) membrane with enhanced flux applied in forward osmosis process. *Journal of Membrane Science*. 375: 63-68.

38. J. Wei, C. Qiu, C.Y. Tang, R. Wang and A.G. Fane. 2011. Synthesis and characterization of flat-sheet thin film composite forward osmosis membranes. *Journal of Membrane Science*. 372: 292-302.

39. L. Dumée, J. Lee, K. Sears, B. Tardy, M. Duke and S. Gray. 2013. Fabrication of thin film composite poly(amide)-carbon-nanotube supported membranes for enhanced performance in osmotically driven desalination systems. *Journal of Membrane Science*. 427: 422-430.

40. L. Setiawan, R. Wang, S. Tan, L. Shi and A.G. Fane. 2012. Fabrication of poly (amideimide)-polyethersulfone dual layer hollow fiber membranes applied in forward osmosis by combined polyelectrolyte cross-linking and depositions. *Desalination*. 312: 99–106.

41. S. You, C. Tang, C. Yu, X. Wang, J. Zhang, and J. Han. 2013. Forward osmosis with a novel thin-film inorganic membrane. *Environmental Science Technology*. 47: 8733–8742.

42. L. Luo, P. Wang, S. Zhang, G. Han and T.S. Chung. 2014. Novel thin-film composite tribore hollow fiber membrane fabrication for forward osmosis. *Journal of Membrane Science*. 461: 28-38.

43. R. C. Ong, T. S. Chung. J. S. d. Wit and B. l. J. Helmer. 2015. Novel cellulose ester substrates for high performance flat-sheet thin-film composite (TFC) forward osmosis (FO) membranes. *Journal of Membrane Science*. 473: 63–71.

44. Q. Jia, Y. Xu, J. Shen, H. Yang and L. Zhou. 2015. Effects of hydrophilic solvent and oxidation resistance post surface treatment on molecular structure and forward osmosis performance of polyamide thin-film composite (TFC) membranes. *Applied Surface Science*. 356: 1105-1116.

45. R. Wang, L. Shia, C. Y. Tang, S. Chou, C. Qiu and A. G. Fane. 2010. Characterization of novel forward osmosis hollow fiber membranes. *Journal of Membrane Science*. 355: 158-167.

46. D. Emadzadeh, W.J. Lau, M. R. Sisakht, H. Ilbeygi, D. Rana, T. Matsuura and A.F. Ismail. 2015. Synthesis modification and optimization of titanate nanotubes polyamide thin film nanocomposite (TFN) membrane for forward osmosis (FO) application. *Chemical Engineering Journal*. 281: 243–251.

47. W.J. Lau, S. Gray, T. Matsuura, D. Emadzadeh, J. Paul Chen and A.F. Ismail. 2015. A review on polyamide thin film nanocomposite (TFN) membranes: History, applications, challenges and approaches. *Water research*. 80: 306 -324.

48. K. Lutchmiah, A.R.D. Verliefde , K. Roest, L.C. Rietveld and E.R. Cornelissen. 2014. Forward osmosis for application in wastewater treatment: A review. *Water research*. 5 8: 1 7 9- 9 7

49. K.Y Wang, Q. Yang, T.S. Chung and R. Rajagopalan. 2009. Enhanced forward osmosis from chemically modified polybenzimidazole (PBI) nanofiltration hollow fiber membranes with a thin wall. *Chemical Engineering Science*. 64:1577-1584.

50. Q. Yang, K.Y. Wang and T.S. Chung. 2009. Dual-layer hollow fibers with enhanced flux as novel forward osmosis membranes for water production. *Environmental Science and Technology*. 43: 2800-2805.

51. E.R Cornelissen, D. Harmsen, K.F. Korte, C.J. Ruiken, J.J. Qin and L.P Wessels. 2008. Membrane fouling and process performance of forward osmosis membranes on activated sludge. *Journal of Membrane Science*. 319: 158–168.

52. N.Y. Yip, A. Tiraferri, W. A. Phillip, J. D. Schiffman and M. Elimelech. 2010. High Performance Thin-Film Composite Forward Osmosis Membrane. *Environmental Science and Technology*. 44: 3812–3818.

53. E.M.G.Castello, J. R. McCutcheon and M. Elimelech 2009. Performance evaluation of sucrose concentration using forward osmosis. *Journal of Membrane Science*. 338: 61–66.

54. S. Lee, C. Boo, M. Elimelech and S. Hong. 2010. Comparison of fouling behavior in forward osmosis (FO) and reverse osmosis (RO). *Journal of Membrane Science*. 365: 34–39.

55. S. Zhao, L. Zou and D. Mulcahy. 2012. Brackish water desalination by a hybrid forward osmosis–nanofiltration system using divalent draw solute. *Desalination*. 284: 175–181.

56. K.L. Hickenbottom, N. T. Hancock, N. R. Hutchings, E. W. Appleton, E. G. Beaudry, P. I. Xua and T. Y. Cath. 2013. Forward osmosis treatment of drilling mud and fracturing wastewater from oil and gas operations. *Desalination*. 312: 60–66.

57. S. Phuntsho, S. Vigneswaran, J. Kandasamy, S. Hong, S. Lee and H. K. Shon 2012. Influence of temperature and temperature difference in the performance of forward osmosis desalination process. *Journal of Membrane Science.* 415:416, 734–744.

58. S. Zhao and L.Zou. 2011. Effects of working temperature on separation performance, membrane scaling and cleaning in forward osmosis desalination. *Desalination*. 278: 157-164.

59. P. Zhao, B. Gao, Q. Yue, S. Liu and H. K. Shon. 2016. Effect of high salinity on the performance of forward osmosis: Water flux, membrane scaling and removal efficiency. *Desalination*. 378: 67-73.

60. N. Akther, A. Sodiq, A. Giwa, S. Daer, H.A. Arafat and S.W. Hasan. 2015. Recent advancements in forward osmosis desalination: A review. *Chemical Engineering Journal*. 281: 502-522.

61. H. Luo, Q. Wang, T.C.Zhang, T.Tao,, AZhou, L Chen and X.Bie A review on the recovery methods of draw solutes in forward osmosis. 2014. *Journal of Water Process Engineering*. 4: 212–223.

62. J. Yaeli. 2992. Method and apparatus for processing liquid solutions of suspensions particularly useful in the desalination of saline water. US Patent 5,098,575.

63. R.L. McGinnis. 2002. Osmotic desalination process, US Patent 6,391,205.

64. J.R. McCutcheon, R.L. McGinnis and M. Elimelech. 2005. A novel ammonia-carbon dioxide forward (direct) osmosis desalination process. *Desalination*. 174: 1-11.

65. S. Adham, J. Oppenheimer, L. Liu and M. Kumar. 2007. Dewatering reverse osmosis concentrate from water reuse using forward osmosis. *Water Reuse Foundation Research*. pp. 1-52.

66. S.K. Yen, F. Mehnas, N. Haja, M. Su, K.Y. Wang and T.S. Chung. 2010. Study of draw solutes using 2-methylimidazole-based compounds in forward osmosis. *Journal of Membrane Science*. 364: 242–252.

67. Q. Ge, J. Su, T.-S. Chung and G. Amy. 2011. Hydrophilic superparamagnetic nanoparticles: synthesis characterization and performance in forward osmosis processes. *Industry Engineering Chemical Research*. 50: 382-388.

68. M.M. Ling, T.S. Chung. 2011. Desalination process using super hydrophilic nanoparticles via forward osmosis integrated with ultrafiltration regeneration. *Desalination*. 278: 194-202.

69. Q. Ge, J. Su, G.L. Amy and T.S. Chung. 2012. Exploration of polyelectrolytes as draw solutes in forward osmosis processes. *Water Research*. 46: 1318-1326.

70. M.M. Ling and T.S. Chung. 2012 Surface-dissociated nanoparticle draw solutions in forward osmosis and the regeneration in an integrated electric field and nanofiltration System. *Industry Engineering Chemical Research*. 51: 15463–15471.

71. K.S Bowden, A. Achilli and A.E, Childress. 2012. Organic Ionic Salt Draw Solutions for Osmotic Membrane Bioreactors. *Bioresource Technology*. 122:207

72. Carmignani, S. Sitkiewitz, and J. W. Webley. 2012. Recovery of Retrograde Soluble Solute for Forward Osmosis. *Water Treatment*. 13: 454-062.
73. R. Ou, Y. Wang, H. Wang and T. Xu. 2013. Thermo-sensitive polyelectrolytes as draw solutions in forward osmosis process. *Desalination*. 318: 48–55.

74. R. Alnaizy, A. Aidan, M. Qasim. 2013. Copper sulfate as draw solute in forward osmosis desalination. *Environmental Chemical Engineering*. 1: 424-4.

75. R. Alnaizy, A. Aidan,M. Qasim. 2013. Draw solute recovery by metathesis precipitation in forward osmosis desalination. *Desalination Water Treatment*. 51: 1-10.

76. Q. Ge, F. Fu and T.S. Chung. 2014. Ferric and cobaltous hydroacid complexes for forward osmosis (FO) processes. *Water Research*. 58:230–238.

77. Zhang, J. Li, H. Cui, H. Li and F. Yang. 2015. Forward osmosis using electric-responsive polymer hydrogels as draw agents: Influence of freezing–thawing cycles, voltage, feed solutions on process performance. *Chemical Engineering*. 259: 814–819.

78. D. Zhao, S. Chen, P.Wang, Q. Zhao and X. Lu. 2014. A dendrimer-based forward osmosis draw solute for seawater desalination. *Industry Engineering Chemical Research*. 53. 16170-16175.

79. Y. Hartanto, S. Yun, B. Jin, S. Dai. 2015. Functionalized thermo-responsive microgels for high performance forward osmosis desalination. *Water Research*. 70: 385-393.

80. E. Tian, C. Hu, Y. Qin, Y. Ren, X.Wang, X.Wang, P. Xiao and X. Yang. 2015. A study of poly (sodium 4-styrenesulfonate) as draw solute in forward osmosis. *Desalination*. 360: 130-137.

81. C.H. Tan and H.Y. Ng. 2012. A novel hybrid forward osmosis - nanofiltration (FO-NF) process for seawater desalination: Draw solution selection and system configuration. *Desalination and Water Treatment.* 13: 356-361.

82. R. Kumar and P. Pal. 2015. A novel forward osmosis-nano filtration integrated system for coke-oven wastewater reclamation. *Chemical Engineering Research and Design.* 100: 542-553.

83. Ratchanok Sungkum. 2009. Characterization of Chitosan Membranes Modified by chemicals, corona and Ar discharge. Master of Science. Prince of Songkla University.

84. N. M. Hidzir, D. J.T. Hill, E. Taran, D. Martin, and L. Grøndahl. Argon plasma treatment-induced grafting of acrylic acid ontoexpanded poly (tetrafluoroethylene) membranes. *Polymer*. 54: 6536-6546.

85. D.E. Weibel, C. Vilani, A.C. Habert and C.A. Achete. 2007. Surface modification of polyurethane membranes using acrylicacid vapour plasma and its effects on the pervaporation processes. *Journal of Membrane Science*. 293: 124–132.

86. H.X. Sun, L. Zhang, H. Chai and H. L. Chen. Surface modification of poly (tetrafluoroethylene) films via plasma treatment and graft copolymerization of acrylic acid. *Desalination*. 192: 271–279.

87. S.Y. Park, H.U. Lee, K. Ahn, J.P. Kim, J.S. Jin, J. Lee, S.Y. Jeong and C.R. Cho. 2011. Enhanced photocatalytic activity of TiO_2-incorporated nanofiber membrane by oxygen plasma treatment. *Thin Solid Films*. 519: 6899–6902.

88. D. S. Wavhal and E. R. Fisher, 2002. Hydrophilic modification of polyethersulfone membranes by low temperature plasma-induced graft polymerization. *Journal of Membrane Science*. 209: 255–269.

89. M. B. Olde Riekerink, G. H. M. Engbers, M. Wessling and J. Feijen. 2002. Tailoring the properties of asymmetric cellulose acetate membranes by gas plasma etching. *Journal of Colloid and Interface Science*. 245: 338–348.

90. D. S. Wavhal and E. R. Fisher, 2003. Membrane Surface Modification by Plasma-Induced Polymerization of Acrylamide for Improved Surface Properties and Reduced Protein Fouling. *Langmuir*. 19: 79-85.

91. L. Zou, I. Vidalis, D. Steele, A. Michelmore, S.P. Low and J.Q.J.C. Verberk, 2011.Surface hydrophilic modification of RO membranes by plasma polymerization for low organic fouling. *Journal of Membrane Science*. 369, 420–428.

92. V. M. Kochkodan and V. K. Sharma. 2012. Graft polymerization and plasma treatment of polymer membranes for fouling reduction: A review. *Journal of Environmental Science and Health, Part A: Toxic/Hazardous Substances and Environmental Engineering*. 47:12, 1713-1727.

93. N. V. Bhat, D. S. Wavhal, 2000. Preparation of Cellulose triacetate pervaporation membrane by ammonia plasma treatment. *Journal of Applied Polymer Science*. 76: 258–265.

94. J. G. Torres, D. Sylla, L. Molina, E. Crespo, J. Mota, and L. Bautista. 2014. Surface modification of cellulosic substrates via atmospheric pressure plasma polymerization of acrylic acid: Structure and properties. *Applied Surface Science*. 305: 292-300.

95. V. Moghimifar, A. Raisia, and A. Aroujaliana. 2014. Surface modification of polyethersulfone ultrafiltration membranes by corona plasma-assisted coating TiO2 nanoparticles. *Journal of Membrane Science*. 461: 69-80.

96. C. Yuenyao, T. Chittrakarn, Y. Tirawanichakul, P. Saeung and W. Taweepreda. 2012. The Effect of argon and oxygen plasma on the surface morphology of Polysulfone membrane. *Thai Journal of Physics*. 8: 41-44.

97. Chalard Yueayao. 2014. Development of a DC plasma system for surface modification of polymeric membrane in gas separation. Doctor of Philosophy. Prince of Songkla University

98. Y. Yu, L. Q. Liu, Z. Q. Tang, M. G. Yan, J. S. Gu and X. W. Wei 2008. Surface modification of polypropylene microporous membrane to improve its antifouling characteristics in an SMBR: Air plasma treatment. *Journal of Membrane Science*. 311: 216–224.

Appendix

Appendix 1. Standard curve conductivity for osmotic pressure

1. Prepare NaCl of 0.5 – 2 M, used NaCl 29.22 g, 58.44 g, 87.66 g and 116.88 g dissolved in 1 L of water.
2. Used conductivity meter analysis

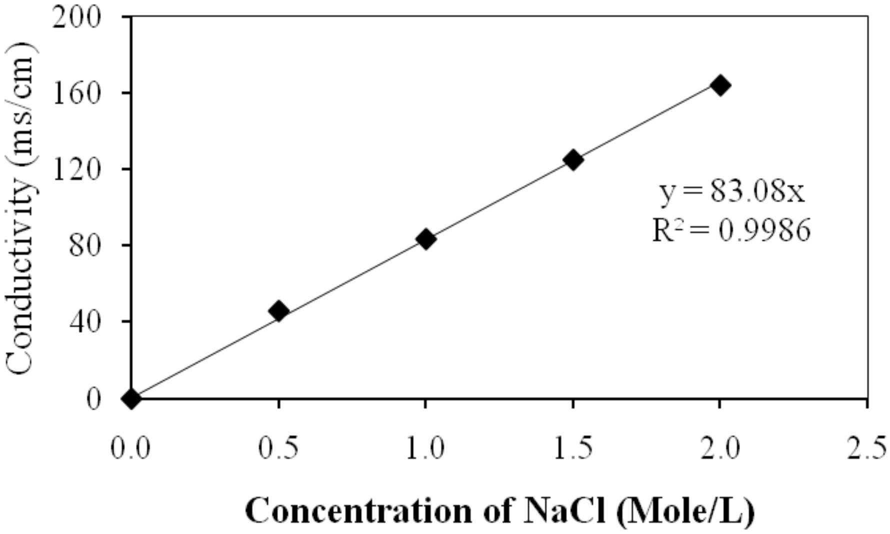

Figure1. Salt standard curve

Appendix 2. Protein analysis Lowry method (Lowry et al., 1995)

Chemical reagent

1. Reagent A. Sodium carbonate (Na_2CO_3) 2 % in 0.1 N Sodium hydroxide (NaOH)
2. Reagent B. $CuSO_4.5H_2O$ 0.5 % in 1 % Potassium tartrate
3. Reagent C. Used solution B 1 ml + solution A 50 ml
4. Reagent D. Used Folin-ciocalteus Phenol reagent dilute 1:1 water

Procedures

1. Prepare of Bovine Serum Albumin (BSA) 0.1 mg/10 (stock solution 1000 ug/ml) dilution at 0, 100
2. Use BSA 200 uL stock solution
3. Add reagent C 2 ml mix solution and incubated at 10 min
4. Add reagent D 0.2 ml mix solution and incubated at 30 min
5. Measured absorbance at 750 nm

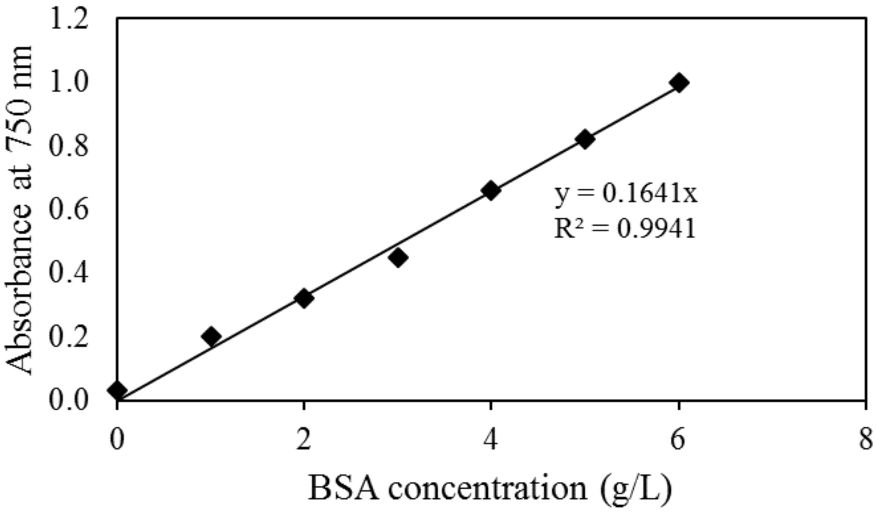

Figure2. BSA standard curve at 750 nm

VITAE

Name Mr. Weerapong Bootluck

Student ID 5510920057

Education Attainment

Degree	Name of Institution	Year of Graduate
Bachelors of Science (Chemistry-Biology)	Prince of Songkla University	2010

List of publication and proceeding

Publication

Watsa Khongnakorn, **Weerapong Bootluck** and Wirote Youravong. 2014. Surface Modification of CTA-FO Membrane by CO_2 Plasma Treatment. *Jurnal Teknologi*.70:2, 71–75.

Proceeding

Bootluck, W., Khongnakorn, W. and Youravong, W. Effect of different concentration of draw solution on BSA recovery by forward osmosis. International Conference on Environmental Engineering, Science and Management. Bangkok, Thailand, March 26-28, 2014.